

Modified zeolite-based polymer nanocomposite membranes for pervaporation

I.G. Wenten^{1,2}, K. Khoiruddin¹, G.T.M. Kadja^{2,3,4},
Rino R. Mukti^{2,3,4} and Putu D. Sutrisna⁵

¹Department of Chemical Engineering, Institut Teknologi Bandung, Bandung, Indonesia ²Research Center for Nanosciences and Nanotechnology, Institut Teknologi Bandung, Bandung, Indonesia ³Division of Inorganic and Physical Chemistry, Institut Teknologi Bandung, Bandung, Indonesia ⁴Center for Catalysis and Reaction Engineering, Institut Teknologi Bandung, Bandung, Indonesia ⁵Department of Chemical Engineering, University of Surabaya (UBAYA), Surabaya, Indonesia

11.1 Introduction

In pervaporation, the membrane is used as a selective barrier for separating feed and permeate streams which are in liquid and vapor phases, respectively. Component to be separated migrates across the membrane and vaporizes while reaches the permeate phase due to vacuum pressure. Pervaporation is mainly applied for the separation of water/organic mixtures, but there are also efforts to utilize this process for desalination [1–7]. As the key factor of the process, attempts have been made to synthesize membrane with desirable separation properties.

Various types of membranes have been developed, such as polymeric, inorganic, and hybrid membranes [8–10]. Polymeric membranes offer numerous advantages, such as economically affordable as well as reasonably good permeability and selectivity. However, using these traditional membranes, one cannot overcome the polymer upper bound between selectivity and permeability which seems to have undergone “saturation” judging from the fact that it only gives a slight increase despite the extensive works which have been devoted for a long time [11–13]. On the other hand, zeolite membranes provide significantly higher permeability and selectivity with other advantages, including superior chemical and thermal stabilities.

Nevertheless, zeolite membranes face an economic barrier because of the higher cost and poor processability. Therefore there should be a breakthrough improvement which combines the advantages of polymer and zeolite inside mixed matrix membranes (MMMs). MMMs are inorganic–organic composites that consist of inorganic materials, in this discussion limited to zeolite, dispersed in an organic polymer matrix as the continuous phase. Aside from combining advantages of both constituents, the production of MMMs actually can be adapted in the current polymer membrane fabrication technology.

Combining the advantages of zeolite and polymer into a membrane means to integrate the molecular sieving and surface diffusion mechanisms within the zeolite membranes with the solution-diffusion mechanism of polymer membranes. Hence, the selectivity and permeability of the MMMs can be further enhanced. It should be noted that the actual performance of MMMs is not a simple combination of the properties of each constituent, but rather it includes many factors which should be taken into account, for example, the particle size and surface area of zeolite and the hydrophobic and hydrophilic nature of zeolite and polymer. The main issue in the fabrication of the MMMs is how to obtain a suitable and strong interaction between zeolite and polymer [8,14,15]. This chapter summarizes the latest development of zeolite-based polymer nanocomposite membranes for pervaporation, including preparation methods, separation performances, water/alcohol separation mechanisms, and challenges of zeolite-filled polymeric membrane fabrication.

11.2 Water and alcohol-selective zeolites

Zeolite is one of the interesting materials for pervaporation since it has uniform pore sizes and tailorable hydrophilic–hydrophobic properties. The uniform molecular pore size allows zeolite to achieve molecular separation with high selectivity. Meanwhile, the tailorable hydrophilic–hydrophobic characteristic provides the possibility to improve the separation factor by increasing the selective sorption toward the permeated component. By combining molecular sieving and selective sorption, the zeolite may achieve an excellent separation performance for pervaporation process [16].

Linde type A (LTA) zeolite is the most used membrane material for pervaporation due to its high separation factor ($\sim 10,000$ for water–ethanol separation) [17]. LTA zeolite comprises aluminosilicates with Si to Al ratio of 1:1, resulting in high

hydrophilicity. The eight-membered oxygen ring creates a maximum pore size of 0.42 nm which is close to the size of a water molecule (kinetic diameter of 0.296 nm [18]). The combination of high hydrophilicity and suitable pore structure enables LTA zeolite for obtaining high water selectivity. Generally LTA zeolite membrane is synthesized by growing LTA zeolite layer on a ceramic support. LTA zeolite membrane can be prepared via primary and secondary growth methods [17]. In primary growth method, the support undergoes hydrothermal processing. Thus, zeolite layer is formed *in situ*. In the secondary growth, the support is firstly coated by zeolite crystals or seeds before the hydrothermal processing step. Even though this type of membrane has high durability and thermal stability, it suffers from several disadvantages, such as high manufacturing cost which is attributed to the cost of support and complex processing steps and low selectivity due to defects formation [17,19]. The application of LTA zeolite for dehydration is also hindered by its hydrothermal stability due to dealumination phenomenon when operated at high water content [20]. Furthermore, the LTA structure is also affected by pH values. Dealumination may occur at acidic environment while operation at basic condition may lead to membrane damage [21,22]. Hence, neutral pH is preferred.

T-type zeolite is another type of zeolite which can be used for pervaporation membrane, especially for dehydration processes. T-type zeolite has Si to Al ratio of 3:1 and 4:1 for erionite and effretite crystals, respectively [23]. The lower content of Al (than LTA) is expected to increase its hydrothermal stability and acid stability, but it yields in lower hydrophilicity. The larger pore size of T-type zeolite framework (0.36 nm × 0.51 nm) leads to lower water selectivity than LTA [24,25]. T-type zeolite membrane has been commercialized by Mitsui Engineering & Shipbuilding Co., Ltd. [26].

Chabazite (CHA) zeolite has a maximum 3D pore size of 0.38 nm or in between of those in KA and NaA LTA zeolites [18]. This yields in an excellent water selectivity and over 270,000 separation factor (Si/Al = ~3; feed: 8% water; 77°C) for ethanol dehydration [27]. In the separation of water/ethanol mixture with 86% water content, CHA with Si/Al of 7.5 can achieve 500 separation factor [28]. CHA zeolite framework may have different Si to Al ratios with the highest of 11:1 [19]. The high Si to Al ratios is believed to improve its organic acid resistance; thus, it can be used for organic acid separation, which is not applicable for LTA. However, the high Si content decreases the water flux of the membrane.

DDR is all-silica zeolite, which is believed as a good alternative for LTA membrane even it is more hydrophobic. The all-silica

Table 11.1 Zeolite type and characteristics.

Zeolite	Characteristics	Reference
LTA	Hydrophilic; pore size: 0.42 nm	[18]
T-type	Hydrophilic; pore size: 0.36 nm × 0.51 nm	[24,25]
CHA	Hydrophilic; pore size: 0.38 nm	[18]
DDR	Hydrophobic; pore size: 0.36 nm × 0.44 nm	[30]
ZSM-5	Hydrophobic; pore size: 0.51 nm × 0.57 nm	[34]

CHA, Chabazite; LTA, Linde type A.

structure makes DDR membrane is more hydrothermally stable than LTA. A long-term pervaporation test on dehydration of acetic acid confirmed that the DD3R zeolite was stable under the presence of inorganic acid [29]. Also, the all-silica DDR membrane displayed good water permeability of $20 \text{ kg m}^{-2} \text{ h}^{-1}$ at 344K–398K and water/ethanol selectivity of 1500 at 373K (0.18 water) [30]. The high silica content and small pore size ($0.36 \text{ nm} \times 0.44 \text{ nm}$) suggest that the separation of water in DDR is based on size exclusion [30]. This is different when compared to the LTA membrane, where water adsorption also occurs.

ZSM-5, which has a mordenite framework inverted (MFI)-type structure, has been studied in developing pervaporation membrane as reported in several works [16,31–34]. In the ZSM-5 framework, the straight channels are elliptical with a pore size of $0.51 \text{ nm} \times 0.57 \text{ nm}$, while the sinusoidal channels have a diameter of 0.54 nm [34]. With that structure, ZSM-5 is also believed as a good selective separator for small molecules. ZSM-5 is alcohol-selective since it has a high Si/Al ratio, which prefers to sorb less polar compound from an aqueous mixture [35]. Silicalite-1 is aluminum-free zeolite, which preferentially adsorbs alcohol [36]. The hydrophobicity of silicalite-1 is similar to ZSM-5 zeolite [36]. These types of zeolite, that is, ZSM-5 and Silicalite-1, are suitable for the preparation of pervaporation membrane used for alcohol removal from aqueous mixtures (Table 11.1).

11.3 Mechanism of water/alcohol separation in zeolite

The successful separation of water/alcohol mixture through the zeolite-filled nanocomposite membranes or MMMs is determined not only by the presence of zeolite particles and polymer

matrices but also by the interaction between zeolite and polymer. To understand the thorough mechanism of water/alcohol separation through the zeolite-filled nanocomposite membranes, the discussion of separation mechanism will be started from the mechanism of separation through the zeolite particles first and then followed by the explanation of separation mechanism through the composite membranes.

11.3.1 The separation mechanism in zeolite particles

The separation of components through zeolite particles can be elucidated by the adsorption of selected component(s) into the pores of zeolites and the diffusion of components along the surface of zeolite mechanisms [18]. In the adsorption process of components to the surface of the adsorbent, the adsorbates or components to be adsorbed are accumulated on the surface of the adsorbent through either physical or chemical adsorption. In the pervaporation process, in which the water/alcohol is mainly separated by composite membranes, physisorption, or physical adsorption dominates the adsorption mechanism of the component in zeolite particles [18]. According to physisorption mechanism, the extent of adsorption can be influenced by the interaction of adsorbent–adsorbate or adsorbate–adsorbate, the pores structure of the adsorbent, and the size of adsorbate molecules.

The adsorption of adsorbate in zeolite particles is commonly quantified using the adsorption isotherm. The adsorption isotherm provides information about the amount of adsorbate adsorbed by adsorbent as the function of relative pressure, the pressure of adsorbate or fugacity at certain temperatures. The adsorption isotherm can be derived from the data of adsorption equilibrium, which is usually expressed in a mathematical model for adsorption equilibrium. Several models have been developed to explain the monolayer and multilayer adsorptions phenomena. For pure component adsorption: Henry's law, Langmuir isotherm, and Freundlich isotherm are common models used to describe the adsorption behavior through the zeolite pores [18,37,38]. Henry's law is usually utilized to designate the adsorption phenomenon at a relatively low pressure, where the adsorption loading is proportional to the adsorption pressure and can be formulated as:

$$q_i = K_{H,i} \cdot p_i, \quad (11.1)$$

where q_i is the surface coverage, p_i is the partial pressure of component or adsorbate, and $K_{H,i}$ is the Henry constant for certain component in adsorbate. At low pressure, the surface coverage of adsorbent by the adsorbate is relatively low, thus produces a linear adsorption isotherm. At high pressure, the direct correlation between adsorption loading and pressure will not be valid. Hence Henry's law is only applicable for low pressure of the adsorption process.

Other models that can be applied to describe the adsorption isotherm through zeolite particles are Langmuir and Freundlich isotherms. The correlation for monolayer Langmuir isotherm is described in Eq. (11.2) [18,38].

$$q_i = \frac{q_{sat,i} \cdot b_i \cdot f_i}{1 + b_i \cdot f_i}, \quad (11.2)$$

where $q_{sat,i}$ is the saturation coverage, b_i is an adsorption equilibrium constant, and f_i is the fugacity of the component where can be substituted by the partial pressure of component for the case of gas adsorption.

The equation for Freundlich isotherm is presented in Eq. (11.3) [18].

$$q_i = K_{F,i} \cdot P_i^n, \quad (11.3)$$

where $K_{F,i}$ and n are the constants that be governed by the nature of the adsorbent and adsorbate at a certain temperature.

The adsorption process in zeolite particles, especially for the low molecular size of adsorbate component, generally follows the Langmuir adsorption isotherm as has been discussed thoroughly in Ref. [18]. For higher molecular size components, the model used to explain the adsorption process can be expanded by using the dual-site Langmuir model.

While the models above have been used extensively to explain the single component adsorption through zeolite pores, the separation of water/alcohol mixture or multicomponent in zeolite pores requires a different model. For water/alcohol mixture, the adsorption mechanism can be elucidated by using extended Langmuir isotherm model, which is formulated in Eq. (11.4) [39],

$$q_i = \frac{q_{sat,i} \cdot b_i \cdot p_i}{1 + \sum_{j=1}^N b_j \cdot p_j}. \quad (11.4)$$

Eq. (11.4) can be applied in the case where the saturation loadings of the mixture are exactly the same. However, in many

cases, the mixture of water/alcohol for separation in zeolite pores is not identical. Hence, for this case, other models should be employed, including the real adsorbed solution theory (RAST) and the ideal adsorbed solution theory (IAST). These two models are distinguished based on the ideality of the adsorbed phase [18,39].

In contrast to the adsorption process, the diffusion of adsorbates into the zeolite particles occurs mainly due to the potential difference within the pores. The extent of the diffusion process is induced by the interactions of the pores wall and the diffusing molecules. It is recognized that the diffusion of adsorbates into the pores of zeolite is a surface diffusion that is influenced by the gradient of the chemical potential of the adsorbates. Generally the diffusion process, along with the porous media, such as zeolite, can be explained using Fick's first law as formulated in Eq. (11.5) [40].

$$J = -D \frac{dC}{dx}, \quad (11.5)$$

where J is the mass transfer flux, D is the diffusion coefficient or diffusivity, dC is the concentration gradient, and x is the position or length.

The Fick's first law shows the correlation between the diffusive flux and concentration under steady-state condition. The flux of component is influenced by the concentration or potential gradient along with the pores of porous media. When the adsorbate is adsorbed to the pores of zeolite, the mobility of the adsorbate could potentially make the adsorbate to jump to different active sites in the pores of the zeolite. This phenomenon requires the adsorbate molecules to surpass some energy barrier that can be represented by Eq. (11.6) [38].

$$D_i = D_i^o \exp\left(\frac{-E_i^{dif}}{RT}\right), \quad (11.6)$$

where D_i is the diffusivity of component i , D_i^o is a preexponential factor, and E_i^{dif} is the activation energy of diffusion. The diffusivity represents the ability of the adsorbate molecules to move, and it can be different among adsorbates. In general, the diffusivity of adsorbate to the pores of zeolite depends on the molecular size of component or adsorbate.

In addition to the adsorption and diffusion mechanisms, the separation of water/alcohol mixture can also be described by the molecular sieving mechanism. This postulation stems from the knowledge of the kinetic diameter of water and alcohol.

The kinetic diameter of water is 0.296 nm, while the kinetic diameters of some alcohol, such as ethanol and methanol are 0.430 and 0.380 nm, respectively [18,41]. The difference in molecular size between water and alcohol could potentially be exploited by finding suitable zeolite with suitable pore size.

11.3.2 The separation mechanism through mixed matrix membranes and inorganic fillers incorporated composite membranes

The water/alcohol separation using pervaporation process is conducted by employing polymeric, inorganic, or hybrid membranes [1,14,31–33,42–44]. In principle, the separation mechanism in pervaporation process is driven by several factors, such as the physical and chemical characteristics of the membranes and the feed solutions, the interactions among the components in the permeants, as well as the interactions between the permeant and membrane. The extent of the separation through the pervaporation membrane can be controlled by controlling the chemical potential gradient, which acts as the driving force for separation. The separation mechanism in pervaporation is mainly described by the solution-diffusion model. However, in some cases, the pore-flow model is also used to explain the separation mechanism [45–47].

In the solution-diffusion model, the separation and the interaction of permeant and membrane are modeled and described by three steps as presented in Fig. 11.1. The first step is the adsorption of liquid feed molecules onto the membrane surface at the feed side and then followed by the diffusion of penetrant through the membrane. The last step includes the desorption of the permeant or permeates at the permeate side [40,48]. In the desorption step, the permeate is in the vapor phase. The flux of the permeate through the membrane can be described by Fick's first law as has been formulated by Eq. (11.5).

The concentration gradient in Eq. (11.5) can be extended to $c'_i - c''_i$, in which c'_i and c''_i are the concentration of component in the feed and permeate sides, respectively. The concentration of the component is the multiplication of vapor pressure (p_i) and the solubility coefficient (S_i) of the component in the membrane. Hence, Fick's first law can be written as [46]:

$$J_i = \frac{D_i \cdot S_i}{\delta} (p'_i - p''_i) = \frac{P_i}{\delta} (p'_i - p''_i), \quad (11.7)$$

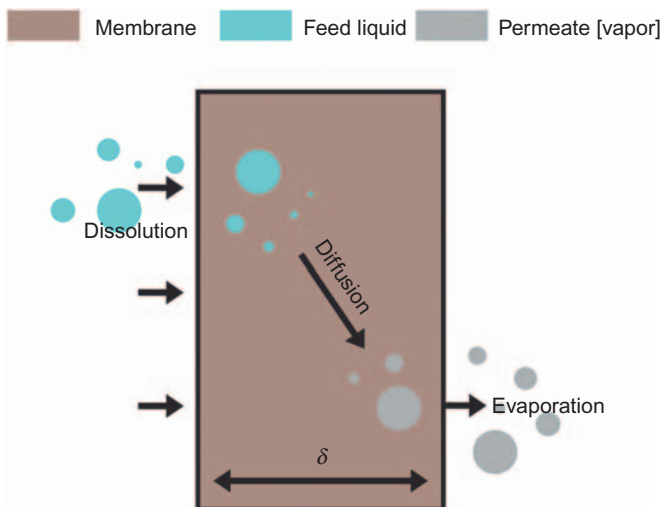


Figure 11.1 The schematic diagram showing the solution-diffusion model.

where $P_i = D_i \cdot S_i$ is the permeability coefficient. In the pervaporation process, the upstream or feed pressure is usually much larger than the permeate pressure, which is vacuum. Also, the concentration of penetrant is much smaller than feed concentration, and the upstream vapor pressure is the saturated vapor pressure (p_i^o); hence

$$J_i = \frac{D_i \cdot c_i}{\delta} = \frac{P_i \cdot p_i^o}{\delta}. \quad (11.8)$$

The successful separation in pervaporation process is measured as the separation factor (α_{ij}). The separation factor is basically the ratio of permeate concentration (y_i/y_j) and feed concentration (x_i/x_j) and can be calculated using Eq. (11.9) [32,43,44,49,50].

$$\alpha_{ij} = \frac{y_i/y_j}{x_i/x_j}. \quad (11.9)$$

As can be seen from Eq. (11.7), the diffusivity and solubility coefficients play important role to determine the extent of the pervaporation process. The solubility coefficient can be predicted by considering three factors, such as the hydrogen bonding interaction, the contribution of polar interaction, and the contribution of dispersion interaction. In water/alcohol separation, the hydrogen bonding interaction between water and alcohol is relatively high. Hence it is concluded that the separation of water from alcohol is feasible using the pervaporation process.

In addition to the solution-diffusion model, the separation of water/alcohol mixture in the pervaporation process can also be explained by the pore-flow model. In contrast to the solution-diffusion mechanism, the phase change in pervaporation is taken in to account in the pore-flow model or mechanism. The schematic diagram showing the pore-flow mechanism is depicted in Fig. 11.2.

The pore-flow mechanism involves three consecutive steps, such as the transfer of liquid from the inner side of the pore to the interface between liquid and vapor, the evaporation process at the boundary of the phase, and the transfer of vapor from the boundary to the outer of the membrane pores. For the mathematical calculation of simple component, it is considered that the flux can be assumed the same in the liquid and vapor regions and can be formulated by using Darcy's law as presented in Eq. (11.10) [51].

$$J_{\text{liquid}} = \frac{A^{\text{pore}}}{l_{\text{liquid}}} (p^{\text{liquid}} - p^{\text{sat}}) = J_{\text{vapor}} = \frac{B^{\text{pore}}}{l_{\text{vapor}}} (p^{\text{sat}} - p^{\text{vapor}}), \quad (11.10.)$$

where A^{pore} is determined by Darcy's equation, B^{pore} is calculated by simplified Henry's law and monolayer adsorption, l_{liquid} is the length of the pore-filled by liquid, p^{sat} is the saturated pressure, and p^{vapor} is the length of pore-filled by vapor.

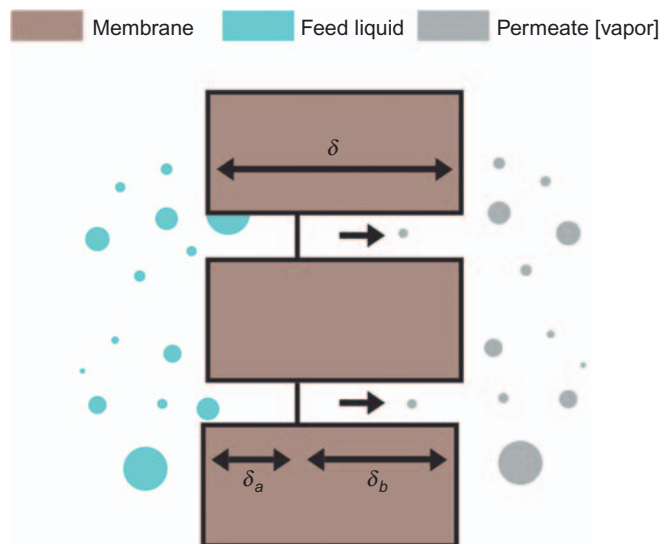


Figure 11.2 The schematic diagram of the pore-flow mechanism.

The extent of water/alcohol separation in pervaporation process is determined by the high values of permeate flux as well as the selectivity of the membranes. In principle, to obtain high flux, it is required to have a thin membrane. The thin membrane will reduce the resistance of mass transfer; however, as experienced by other membrane processes, there is also a trade-off between the flux and selectivity of the membranes. To produce a high flux through the membranes, we can employ a composite membrane that has a thin active layer and porous substrate. The thin layer acts as the separating layer and is usually in the form of a dense layer. On the other hand, the porous substrate provides an enhancement in the mechanical strength of the composite membrane. In recent years, the thin layer of pervaporation membrane has been synthesized by combining the polymer matrix and inorganic particles [14,43]. This combination tries to exploit the separation capabilities of both materials. In another line of research, the application of MMMs in pervaporation has just been started recently. In MMMs, the inorganic fillers, such as zeolite particles, are incorporated inside the polymer matrix. Hence, the separation mechanism inside the membranes will combine the separation mechanism of pure zeolite and pure polymeric materials.

The successful pervaporation process using composite membranes and MMMs is determined mainly by the absence of voids and defects on the interface between the inorganic fillers and the polymer matrix. Voids and defects in polymer–particle combination in some cases can increase the flux through the membranes but will decrease the selectivity of the membranes. The formation of void and defect-free composite membranes and MMMs is therefore growing as an interesting field of research in the pervaporation process. The different morphologies of polymer–particles will determine the separation mechanism through the composite membranes, and MMMs are depicted in Fig. 11.3. The morphologies include ideal morphology, sieve-in-a-cage, the rigidification of polymer, and the blockage of particle pore [42,52,53]. These defects can be caused by several factors, such as the incompatibility between polymer and particle, the evaporation of solvent during membrane formation that stresses the interface of polymer–particle, and the weak adhesion between the particle and polymer [54].

As has been mentioned and presented in Fig. 11.3, four morphologies or cases in MMMs can be described as (1) idealized or “hard to obtain” morphology, (2) rigidified polymer layer morphology, (3) reduced permeability region within sieve morphology, and (4) voids at the interface morphology.

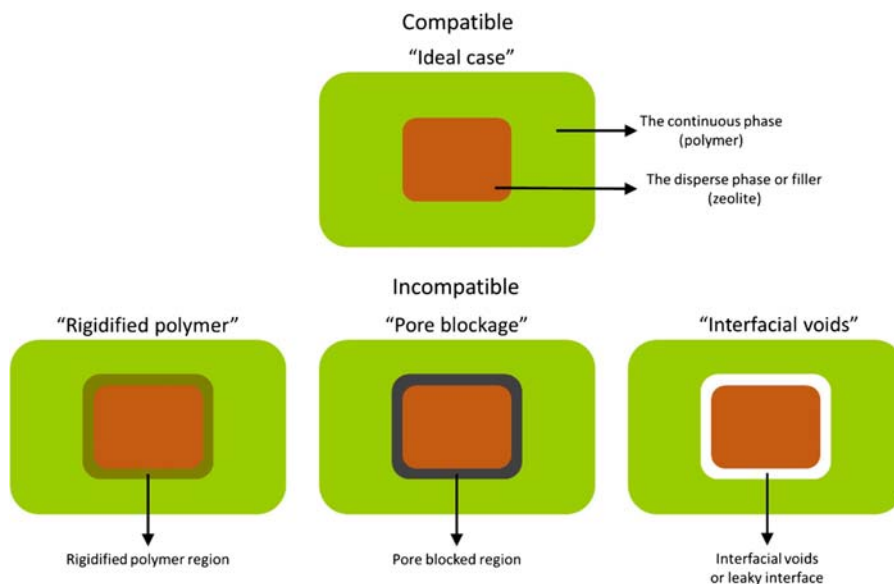


Figure 11.3 The morphologies and typical defects in MMMs. *MMM*s, Mixed matrix membranes.

Case 1 is usually explained by Maxwell model that is formulated by Eq. (11.11):

$$P_{mm} = P_c \left(\frac{P_d + 2P_c - 2\phi_d(P_c - P_d)}{P_d + 2P_c + \phi_d(P_c - P_d)} \right), \quad (11.11)$$

where P_{mm} is the effective permeability of an MMMs, ϕ is the volume fraction, while c and d denote the continuous and dispersed phases, respectively.

Case 2 demonstrates the formation of the rigidified region on the interface between the polymer matrix and inorganic particles. The rigidified region arises because of the stress experienced by two materials during the preparation of MMMs. When the rigidification of polymer occurs, it can be expected that polymer layer near the particle surface has low chain mobility that will improve the resistance to penetrants and will decrease the permeability and increase the membrane selectivity. This phenomenon can be observed by the increasing value of the glass transition temperature of the polymer. In case 3, the interface between polymer matrix and inorganic particles has a region with reduced permeability in the outer layer of the particles or the whole particles. In case 4 or sieve-in-a-cage morphology, membrane shows in increased permeability with the

negligible change of the selectivity. Although this morphology is favorable, it will be difficult to synthesize such morphologies without a significant loss of selectivity.

11.4 Fabrication of zeolite-filled nanocomposite membranes

In the preparation of hybrid inorganic/organic membrane, the following suggestions should be considered [55,56]:

- The inorganic filler should be small, well distributed in the polymer matrix, and no aggregation. In some cases, when the filler requires activation, the temperature should be suitable for the polymer stability.
- The procedure for the preparation of polymer matrix should allow the particle to be easily dispersed in the polymer matrix.
- Nanoparticles and polymer should have high compatibility to avoid the defect formation in the interfacial of nanoparticle and polymer.

One of the important factors in the preparation of zeolite-filled nanocomposite membranes is zeolite loading. Zeolite membrane plays an important role in improving membrane selectivity. Thus, the selectivity would be proportional to zeolite content. However, more zeolite content will result in a loose membrane structure or more free volume in the membrane matrix [8]. The formation of more free volume may be associated with the weak interfacial adhesion between zeolites and the polymer matrix. This is undesirable because it will yield a considerable decrease in membrane separation factor even though the membrane will have a higher permeate flux.

Inorganic/organic membranes can be prepared via several methods, such as blending, layer-by-layer self-assembly, in situ polymerization, sol-gel, and bioinspired methods [10,14,57–60]. In the blending method, inorganic particles were dispersed in a polymer solution before casting. Layer-by-layer assembly method consists of multilayer deposition of a selective layer on a support. In general, the layers are polyelectrolytes having positive or negative charges [61]. Polyelectrolytes are then deposited in multitudes on the membrane support. The compatibility between the layers is facilitated by electrostatic interaction of the charge. The sol-gel method involves the hydrolysis and polycondensation reactions of the inorganic precursors. These reactions take place in the polymer solution, and thus simultaneous polymer solidification and nanoparticles formation occur that form inorganic/polymer hybrid membrane.

Unlike the blending method, in situ polymerization uses monomers instead of the polymer [31]. After the monomer and inorganic particles are mixed to form a homogenous solution, the solution undergoes polymerization. In this method, fillers are entrapped in the polymer matrix during the polymerization; thus, a well-dispersed filler is attained. Bioinspired method for fabricating organic–inorganic membrane involves the biomineralization process. For the biomineralization process, the biomineralizing agent made from biological or synthetic molecules and precursors such as inorganic salts or alkoxide molecules are used. Since biomineralization is carried out at the molecular level, uniform distribution of inorganic fillers can be attained. This also provides the possibility of controlling the inorganic filler size, structure, and chemical composition as well as interfacial interaction between the inorganic filler and polymer matrix. Among the methods above, blending is the most common and simplest method for fabricating inorganic-filled polymeric membrane. In general, different techniques to blend zeolite particles and polymeric solution include simple blending, zeolite blending followed by in situ polymerization, zeolite blending followed by cross-linking, and zeolite blending followed by heat treatment as illustrated in Fig. 11.4.

Pervaporation membranes are typically fabricated into tubular and flat-sheets configurations. Zeolite nanoparticles can be incorporated into the membrane matrix by simply blending the particles into a polymer solution before casting to form a membrane. This method is suitable for the preparation of a flat sheet membrane. The membrane solution can be cast directly to form a free-standing membrane or cast on porous support to create a composite membrane. In the composite membrane, the cast membrane acts as the selective layer while the support improves the mechanical strength of the membrane—for instance, Guan et al. [62] fabricated zeolite/poly(vinyl) alcohol (PVA) membrane by preparing a suspension of zeolite/PVA aqueous solution. Fumaric acid, which acted as a cross-linking agent, was added to the suspension. After rigorous mixing, the suspension was cast on nonwoven fabric substrate fixed on a glass plate. When the phase inversion process was completed, the membrane was then heated in the oven at 150°C to induce cross-linking reaction. The pervaporation of 80% ethanol/water mixture at 60°C revealed that the cross-linking procedure successfully improved the membrane selectivity from 511 (for noncross-linked membrane) to 1297. The enhanced selectivity was attributed by the decrease of the polymer's free volume due to the cross-linking reaction [8].

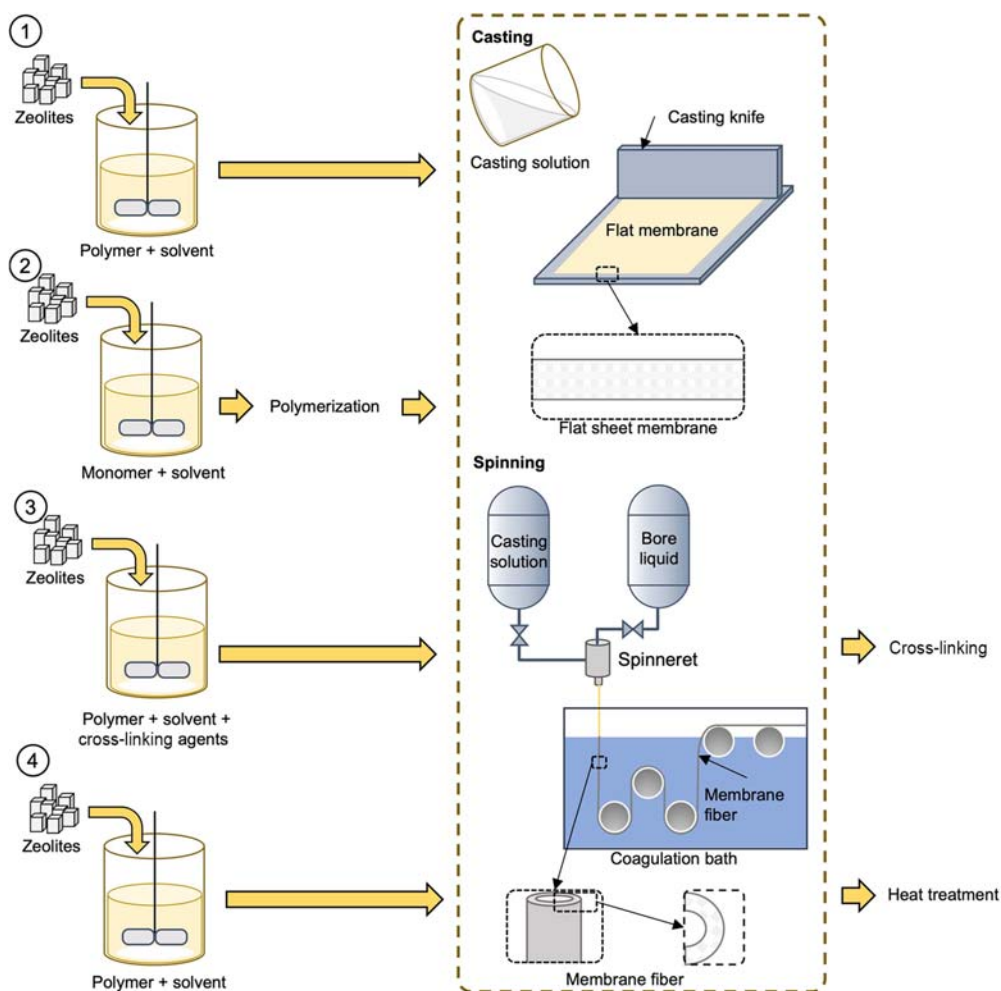


Figure 11.4 The illustration of blending method. (1) Zeolite blending, (2) zeolite blending followed by in situ polymerization, (3) zeolite blending followed by cross-linking, and (4) zeolite blending followed by heat treatment.

The effect of polymer cross-linking on zeolite/polymer membrane was also investigated by Zhan et al. [31] for the synthesis of zeolite/PDMS membrane. They prepared a suspension containing zeolite, PDMS prepolymer, and *n*-hexane by stirring and ultrasonication treatment. Ultrasonication is usually aimed to improve the dispersion of particles and to avoid the agglomeration of nanoparticles during the preparation of the membrane casting solution [63–68]. Cross-linking agent, poly(phenyltrimethoxysiloxane) (PTMOS), and catalyst, di-*n*-butyltin dilaurate, were added into the suspension. These reagents were used

to induce the prepolymerization reaction of PDMS. The suspension was then cast on porous PVDF membrane support and dried subsequently. To obtain the complete cross-linking, the membrane was placed in an oven at 80°C for 5 h. One such problem that usually occurs during the fabrication of zeolite-filled membrane is the agglomeration of filler or zeolites. However, in this study, SEM characterization of the synthesized membrane showed no agglomeration of nanoparticles in the membrane matrix. Meanwhile, the cross-linking procedure could produce a membrane with better selectivity. However, the selectivity was dramatically reduced when the zeolite content was above 30%. They concluded that higher zeolite content would destroy the interfacial adhesion between zeolite particles and the polymer matrix.

During the membrane fabrication process, heat treatment can be utilized to improve the separation properties of the synthesized membrane. Ahmad and Hägg [69] examined the effect of pretreatment and posttreatment on the properties of zeolite 4A/polyvinyl acetate membrane. Zeolite-filled membrane prepared from calcined zeolite displayed improved permeability, selectivity, and thermal stability. The improved performance of produced membranes was attributed by the strong adhesion of zeolite/polymer due to the removal of adsorbed water from the zeolite during the calcination process at 500°C. They also found that the annealing of the prepared membrane could improve membrane selectivity but reduce its permeability. The loss of membrane permeability after annealing at higher temperature might be due to the formation of more rigid membrane structure. Therefore, they suggested to optimize the annealing temperature for improving membrane selectivity at reasonable flux.

The preparation of zeolite/polymer membrane using the layer-by-layer method has been demonstrated by Kang et al. [61]. The layer-by-layer method was successfully used to synthesize zeolite-filled polymer membrane with relatively high particle loading between 30 and 60 wt.%. The membrane was prepared by the deposition of negatively charged poly(acrylic acid), positively charged polyethyleneimine, and LTA zeolite particles on polyacrylonitrile. The LTA zeolite was endowed with negative charge to improve zeolite/polymer compatibility. The electrostatic interactions between those components made the layer highly compatible.

Tubular-type membrane, especially hollow fiber membrane, could provide higher packing density than other configurations. Hence pervaporation plant will have lower footprint. Hollow fiber membrane can facilitate better contact between the liquid

phase in the feed and vapor phase in the permeate. Spinning technique can be used to prepare hollow fiber zeolite/polymer membrane. Ge et al. [70] synthesized zeolite/polymer-based hollow fiber membrane by firstly blending zeolite crystals into a polymeric solution. Then, polyethersulfone solution containing LTA zeolite crystals were spun to form hollow fiber membrane with 2.2 mm and 1.0 mm outer diameter and inner diameter, respectively. The composite hollow fiber membrane showed $>10,000$ selectivity and $9000 \text{ g m}^{-2} \text{ h}^{-1}$ in the pervaporation of 90% ethanol solution conducted at 60°C .

11.5 Zeolite–polymer compatibility

As the performances of zeolite/polymer composite membranes are affected by the compatibility of the zeolite particles and polymer materials, this section presents several aspects related to the issue of polymer–particles compatibility.

11.5.1 Predicting the combination of zeolite and polymer

To predict the permeability of the MMMs, several analytical models can be utilized. One of the most popular models is the Maxwell model or equation as presented in Eq. (11.12) [71,72].

$$P_i^M = P_i^P \left(\frac{P_i^Z + 2P_i^P - 2\phi(P_i^P - P_i^Z)}{P_i^Z + 2P_i^P + \phi(P_i^P - P_i^Z)} \right), \quad (11.12)$$

where P_i^M , P_i^P , and P_i^Z are the permeability of component i in the MMMs, polymer, and zeolite, respectively, while ϕ is the volume fraction of the zeolite. This model assumes the zeolite particle to be spherical with a low to moderate concentration ($\phi < 0.3$). Another model developed by Cussler considers the nonspherical shape of the zeolite which increases the tortuosity of the diffusion path with a moderate to high concentration ($\phi > 0.3$). The Cussler model is shown in Eq. (11.13).

$$P_i^M = P_i^P \left(\frac{1}{1 - \phi + \left(\frac{1}{(1/\phi)(P_i^Z/P_i^P) + 4((1-\phi)/\alpha^2\phi^2)} \right)} \right), \quad (11.13)$$

where α is the zeolite aspect ratio or the ratio between the longest and the shortest dimension of zeolite particle. It should be stressed out that Cussler defines α as half of this ratio. Hence,

the equation differs accordingly. Cussler model is reasonably accurate when α is large. However, there are many combinations of α and ϕ in which Maxwell and Cussler model cannot successfully predict the MMMs performance. For this reason, the Cussler model is modified to fill other α and ϕ combinations, as depicted in Eq. (11.14).

$$P_i^M = P_i^P \left(\frac{1}{1 - \phi + \left(\frac{1}{(1/\phi)(P_i^Z/P_i^P) + ((1-\phi)/\alpha^2\phi^2)} \right)} \right). \quad (11.14)$$

In all models, the selectivity can be calculated as P_i^M/P_j^M . For example, we have a certain polymer, so-called polymer I, with a CO_2 permeability and a CO_2/CH_4 selectivity of 20 Barrer and 20, respectively. We need to select the proper zeolite for the filler between zeolite C (CO_2 permeability = 60 Barrer, CO_2/CH_4 selectivity = 100) and zeolite D (CO_2 permeability = 700 Barrer, CO_2/CH_4 selectivity = 80). Suppose the volume fraction of zeolite to be 30%, we can predict the performance of the resulted MMMs, membrane I-C and I-D. Using the Maxwell model, it is seen that membrane I-C exhibits substantially higher selectivity than that of membrane I-D and pure polymer I (Fig. 11.5).

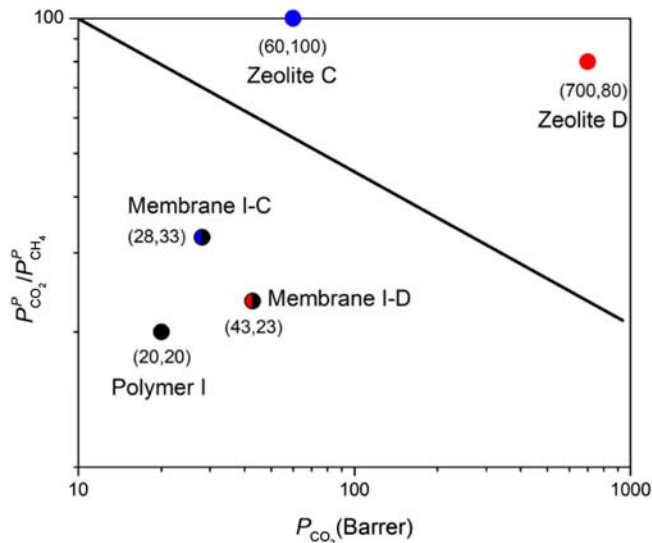


Figure 11.5 Selecting a decent zeolite for mixed matrix membranes based on the Maxwell equation. The black line indicates the polymer upper-bound limit.

Hence, zeolite C is preferred than zeolite D as a filler to form MMMs with polymer I. Cussler and modified Cussler models can be used when another parameter, that is, the aspect ratio, is known.

11.5.1.1 *Toward compatible zeolite–polymer mixed matrix membranes*

The main concern in the preparation of zeolite–polymer MMMs is the compatibility between the zeolite and the polymer. The zeolite should be compatible with the continuous matrix so that the resulted MMMs are free of defects. This means full-coverage of the zeolite by the polymer as well as “just right” adhesion forces between these two phases, which is the ideal case. Incompatibility between the zeolite and the polymer could be, at least, three cases [53]. As depicted in Fig. 11.4, the first case (1) occurs through the densification of the polymer network at the interface resulted in a rigidified region. In this case, the permeability is reduced with or without increasing the selectivity according to the extent of rigidification. In the MMMs of polyethersulfone (PES) and zeolite A for O₂ and N₂ separation, it is predicted through the Maxwell equation that the permeability should increase with the addition of more zeolite A [73]. However, the actual experiments showed the opposite that the permeability decreased with the increase in zeolite loadings. It was found that the results were owing to the occurrence of polymer rigidification since the glass temperature (T_g) of the MMMs was higher than that of the pure PES. Zarshenas et al. [74] reported that in spite of the increase in selectivity, the polyether block amide (Pebax-1657)–nanozeolite X MMMs showed a decline in the gas permeability for the separation of CO₂ from N₂, and O₂. This was also indicated by the increased of T_g after the addition of zeolite. The rigidification of polymer networks in the MMMs has also been reported by other researchers [75–78].

The second case (2) is when the polymer networks penetrate into the pore structure of zeolite, which block the pathway for the desired molecules. This situation leads to the suppressed molecular sieving functionality of zeolite, and hence the selectivity may be kept constant, but the permeability reasonably decreases. The first- and second cases are relatively difficult to be discriminated. Even, they are often found to occur simultaneously within the MMMs [73,79,80].

The third case (3), the most often to occur, is due to the low adhesion leading to the formation of defects and empty

interfacial voids which have a larger size compared to that of zeolite micropores. Consequently the penetrant molecules can easily pass through those voids, making no use of the zeolite. The permeability enhances significantly with the decrease in gas selectivity. Mahajan et al. [81] performed a comparative study on the preparation of MMMs using zeolite 4A as the filler and polyvinyl acetate (PVAc) and commercial polyimide (Matrimid) as polymer matrices. They found that PVAc could provide a full-coverage to zeolite A while Matrimid–zeolite A membranes displayed the observed leaky interface or the interfacial voids. The latter case was due to the incompatibility of Matrimid with the surface of zeolite 4A (Fig. 11.6). The nature of Matrimid is comparatively hydrophobic owing to the presence of both aliphatic and aromatic chains. On the other hand, zeolite 4A possesses hydroxyls (–OH) on its surface, which are relatively hydrophilic. Hence, their interaction is unfavorable, which leads to poor adhesion.

It is crystal clear that the compatibility between zeolite, as the dispersed phase, and polymer, as the continuous phase, depends on the nanoscale morphology at the interface and dictates the performance of the MMMs (Fig. 11.7). The previously described analytical methods, that is, Maxwell, Cussler, and modified Cussler methods work accurately for the ideal case. Nevertheless, under the nonideal cases, they fail to accurately predict the performance of MMMs. The strategies to overcome the incompatibility issues rely on the use of either inorganic or organic agents to bridge the polymer and the zeolite.

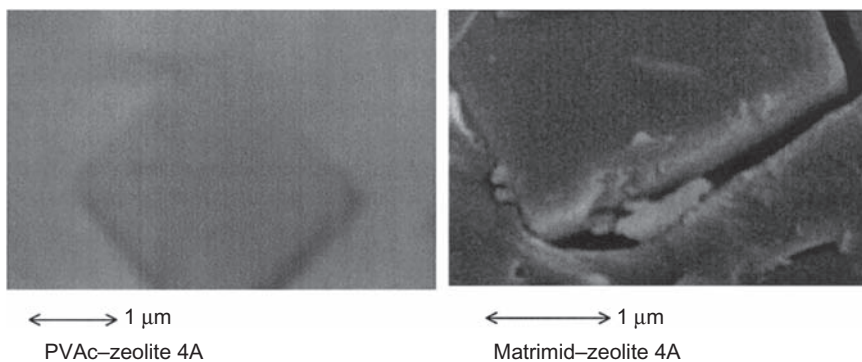


Figure 11.6 Cross-sectional SEM images of PVAc–zeolite 4A and Matrimid–zeolite 4A mixed matrix membranes. *Source:* Reprinted with the permission from R. Mahajan, R. Burns, M. Schaeffer, W.J. Koros, Challenges in forming successful mixed matrix membranes with rigid polymeric materials, *J. Appl. Polym. Sci.* 86 (2002) 881–890, Copyright John Wiley & Sons.

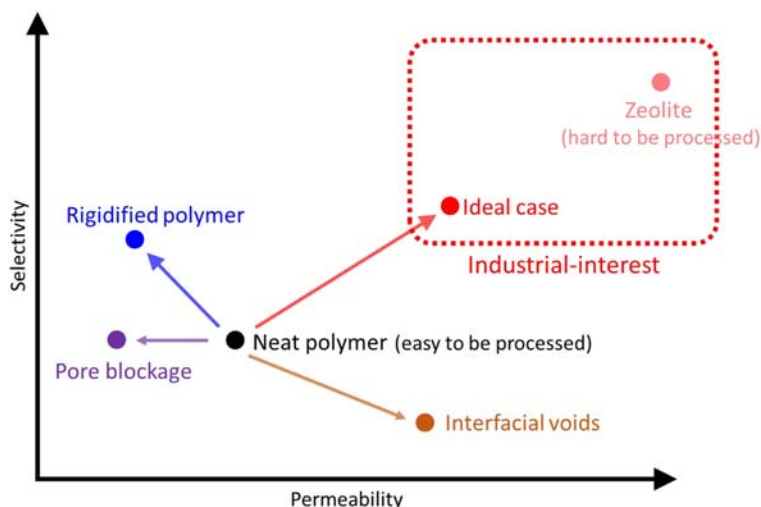


Figure 11.7 The performance of mixed matrix membranes as a function of their morphology.

11.5.1.2 Inorganic bridging agents

The use of inorganic agents to bridge the polymer and the zeolite has attracted attention due to its simplicity and ability to enhance the performance of MMMs. Specifically MgO_xH_y nanoparticles, where $1 \leq x \leq 2$ and $0 \leq y \leq 2$, have been used in this purpose. There are, at least, four methods to grow MgO_xH_y nanoparticles on the surface of zeolite as shown in Fig. 11.8. Through the Grignard method, the Grignard reagent (alkyl magnesium bromide) is hydrolyzed to create MgO_xH_y nanoparticles on the surface of zeolite [82,83]. In this method, the zeolite would undergo a pretreatment either delamination or seeding using thionyl chloride or sodium chloride, respectively. Through the solvothermal method, MgO_xH_y nanoparticles are grown in the presence of a simple organic solvent, that is, ethylenediamine, water, and Mg^{2+} ions at a high temperature and autogenous pressure [84,85]. This method could be modified using a bulkier organic solvent such as diethylenetriamine to prevent the zeolite micropores to be penetrated by the solvent [85]. The last method, that is, the ion-exchanged method, includes the ion exchange of Na^+ ion residing in the zeolite structure with Mg^{2+} at a neutral pH, followed by a hydrothermal treatment under Na^+ solution at a basic pH (9.5) [86]. At the latter stage, reverse ion exchange takes place along with the formation of MgO_xH_y nanoparticles on the surface of the zeolite. Lydon et al. [56] have examined the four said methods to prepare MMMs from Matrimid and zeolite LTA. They showed that the MMMs prepared without bridging agents resulted in the formation of

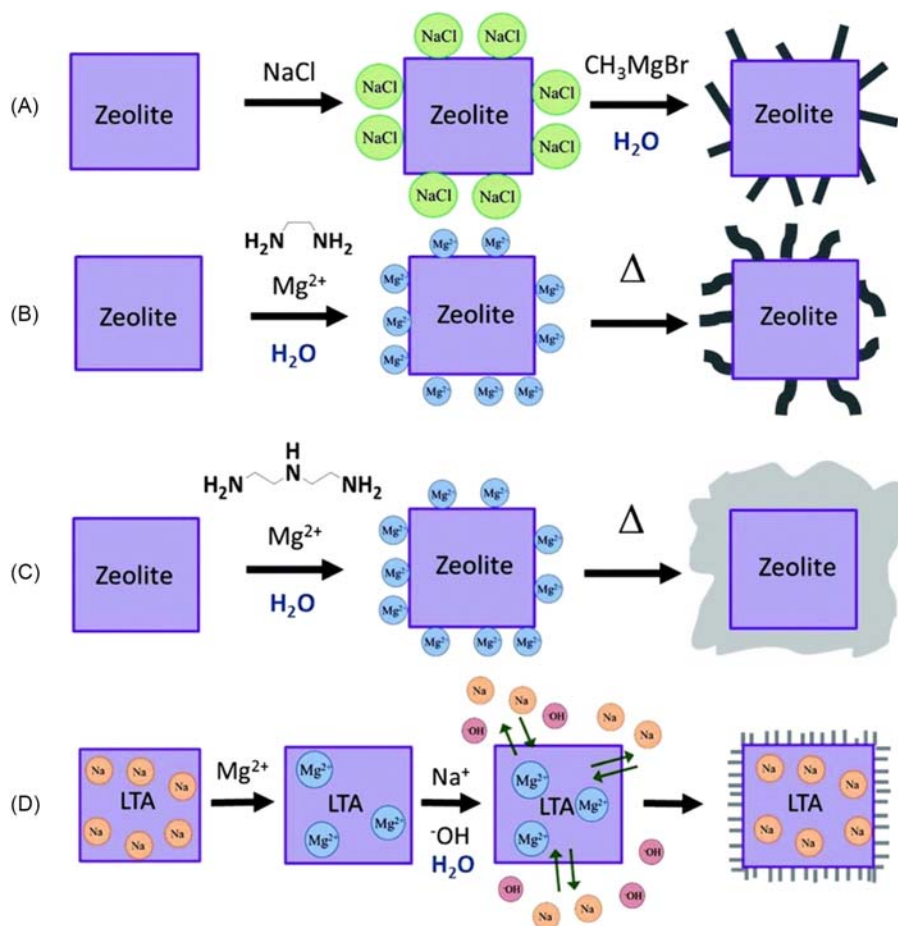


Figure 11.8 Synthesis of MgO_xH_y nanoparticles on the surface of zeolite via (A) Grignard, (B) solvothermal, (C) modified solvothermal, and (D) ion-exchange methods. *Source:* Reprinted with the permission from M.E. Lydon, K.A. Unocic, T.-H. Bae, C.W. Jones, S. Nair, Structure–property relationships of inorganically surface-modified zeolite molecular sieves for nanocomposite membrane fabrication, *J. Phys. Chem. C* 116 (2012) 9636–9645, Copyright American Chemical Society.

interfacial voids while the ones prepared using inorganic bridging agents displayed full-coverage and good adhesion as depicted in Fig. 11.9. The nanoparticles could enhance the area of zeolite and played a role as interlocks to strongly bind the polymer and the zeolite.

Shu et al. [82] prepared the MMMs using a poly(ether imide), so-called Ultem, and zeolite 4A. It was shown that the interfacial voids were formed due to the incompatibility between the dispersed and continuous phases, which caused a decrease in selectivity. Incorporating MgO_xH_y nanoparticles on the surface

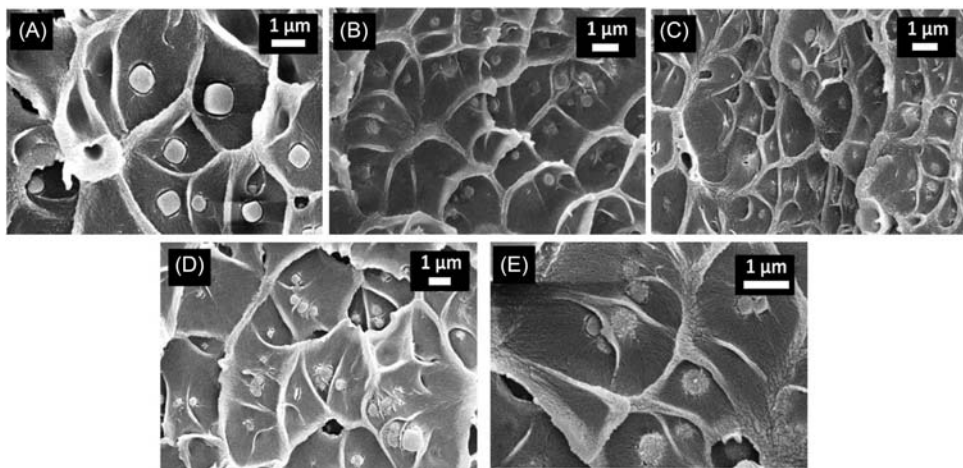


Figure 11.9 Matrimid/zeolite LTA mixed matrix membranes prepared (A) without the presence of bridging agents and with the presence of MgO_xH_y nanoparticles prepared via (B) Grignard, (C) solvothermal, (D) modified solvothermal, and (E) ion-exchange methods. *Source:* Reprinted with the permission from M.E. Lydon, K.A. Unocic, T.-H. Bae, C.W. Jones, S. Nair, Structure–property relationships of inorganically surface-modified zeolite molecular sieves for nanocomposite membrane fabrication, *J. Phys. Chem. C* 116 (2012) 9636–9645, Copyright American Chemical Society.

of zeolite 4A through the Grignard method led to the elimination of the interfacial voids. Consequently the permeability and selectivity substantially improved in the separation of O_2/N_2 as well as CO_2/CH_4 . Ultem was also not compatible with zeolite MFI; however using MgO_xH_y nanoparticles as a bridge prepared via the solvothermal method, the defect-free MMMs could be realized [85]. The resulted MMMs showed an enhancement in gas permeability and selectivity during CO_2/CH_4 separation.

From the thermodynamic point-of-view, the compatibility of the zeolite and the polymer is entropy-driven. In general, the polymer prefers the random coils as its conformation. When the polymer sticks or adsorbs on the surface of zeolite assumed to be flat and smooth, it should adapt by deforming into a more ordered shape. In this way, the entropy change (ΔS) is highly negative. If the enthalpy change (ΔH) is not negative enough to offset the $-T\Delta S$ part, the Gibbs free energy (ΔG) will be >0 . Thus the process cannot occur spontaneously. Note that the Gibbs free energy is expressed as $\Delta G = \Delta H - T\Delta S$. The presence of inorganic bridges at the surface of zeolite increases the surface heterogeneity so that the polymer does not have to deform the confirmation to a far extent. At this condition, ΔS is less negative compared to the adsorption on a smooth surface. Hence, ΔG could be >0 , which means spontaneous adsorption.

11.5.1.3 Organic bridging agents

The most widely known that organic bridging agents are the organosilanes which work by covalently bound to the hydroxyl groups on zeolite surface through the silylation reaction to form siloxane bondings while the other functional groups either react to form covalent bonds or strongly interact with the polymer. In general, the organosilanes acting as organic bridging agents include 3-aminopropyl-triethoxy silane (APTES), *N*- β -(aminoethyl)- γ -aminopropyltrimethoxy silane, γ -glycidyloxypropyl-trimethoxy silane, and 3-aminopropyl-dimethyl ethoxy silane [87]. Ismail et al. [87] prepared the PES–zeolite 4A MMMs using APTES as the bridging agent. The schematic diagram in Fig. 11.10 shows the bridging role of APTES. Without the use of organosilanes, the interfacial voids were observed while those voids were eliminated when the organosilanes were utilized (Fig. 11.11). The defect-free MMMs consisted of polyimide (6FDA-6FpDADABA) and APTES-functionalized zeolite L was prepared by Pechar et al. [88]. The performance test on the separation of N_2/CH_4 showed an increase in both permeability and selectivity. It should be stressed out that the use of organosilanes cannot be too excessive since they can penetrate into the zeolite porosity or create too many linkages which result in pore-blockage.

Aside from organosilanes, other types of organic compounds could also be used with the prerequisite of being able to strongly interact with both zeolite and polymer, typically via the hydrogen bonds. Yong et al. [89] demonstrated the use of 2,4,6-triaminopyrimidine as an effective bridge for defect-free

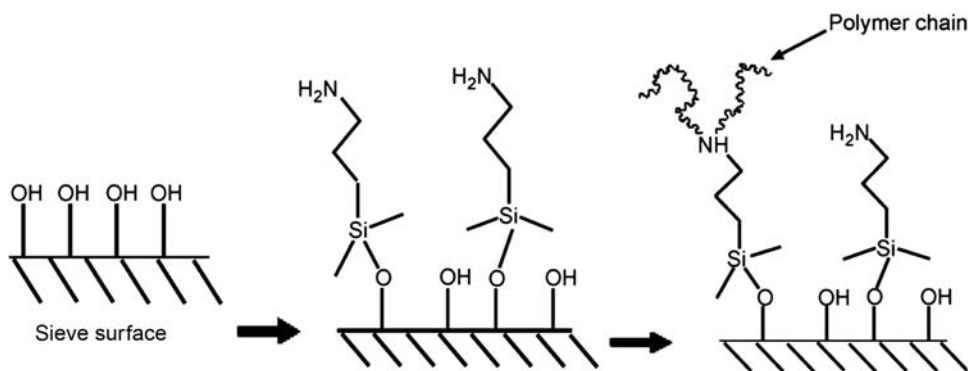


Figure 11.10 The role of organosilanes to bridge zeolite and polymer in the mixed matrix membranes.

Source: Reprinted with the permission from A.F. Ismail, T.D. Kusworo, A. Mustafa, Enhanced gas permeation performance of polyethersulfone mixed matrix hollow fiber membranes using novel Dynasylan Ameo silane agent, *J. Memb. Sci.* 319 (2008) 306–312, Copyright Elsevier.

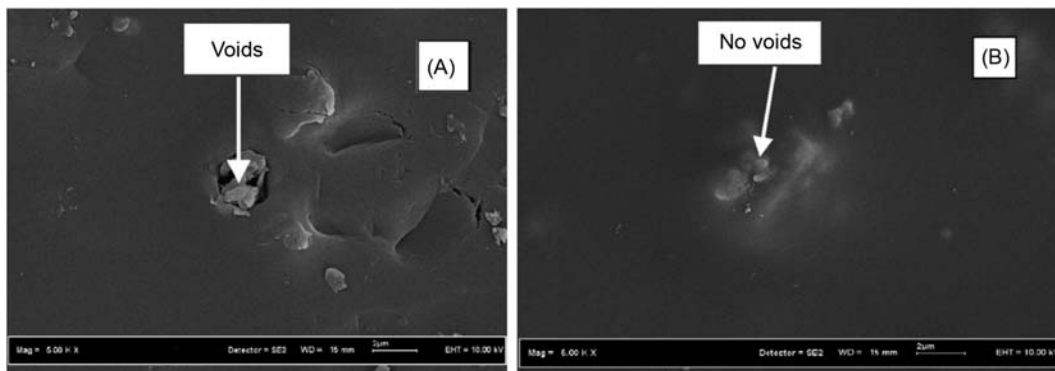


Figure 11.11 Mixed matrix membranes of PES–zeolite 4A (A) without and (B) with organosilanes. *Source:* Modified and reprinted with the permission from A.F. Ismail, T.D. Kusworo, A. Mustafa, Enhanced gas permeation performance of polyethersulfone mixed matrix hollow fiber membranes using novel Dynasylan Ameo silane agent, *J. Memb. Sci.* 319 (2008) 306–312, Copyright Elsevier.

Matrimid-based membranes with various type of zeolites (Fig. 11.12). Matrimid-2,4,6-triaminopyrimidine–zeolite-13X showed a CO_2/CH_4 selectivity of 617, which was a remarkable enhancement since the selectivity of pure Matrimid was only 1.22. Matrimid-2,4,6-triaminopyrimidine–zeolite 4A also displayed another dramatical increase in CO_2/CH_4 selectivity of 133. However, both cases showed a decline in gas permeability.

11.5.1.4 Alternative strategies for improving compatibility

There are other strategies to prepare the defect-free MMMs aside from using the bridging agents. One of the simplest alternatives is priming method. In this method, zeolite is modified using a dilute polymer solution to introduce an ultrathin layer of either the same polymer or different to the matrix polymer [90]. This method could increase the adhesion and prevent the particle agglomeration, especially when the zeolite is in nano-sized range. Another strategy is by annealing at the temperature higher than the polymer T_g to render the polymer to be more flexible for better contact and interaction with the zeolite [91].

11.6 Zeolite–polymer membrane performances in pervaporation

Pervaporation is generally used for organic solvent dehydration and alcohol removal from aqueous mixtures. Performances

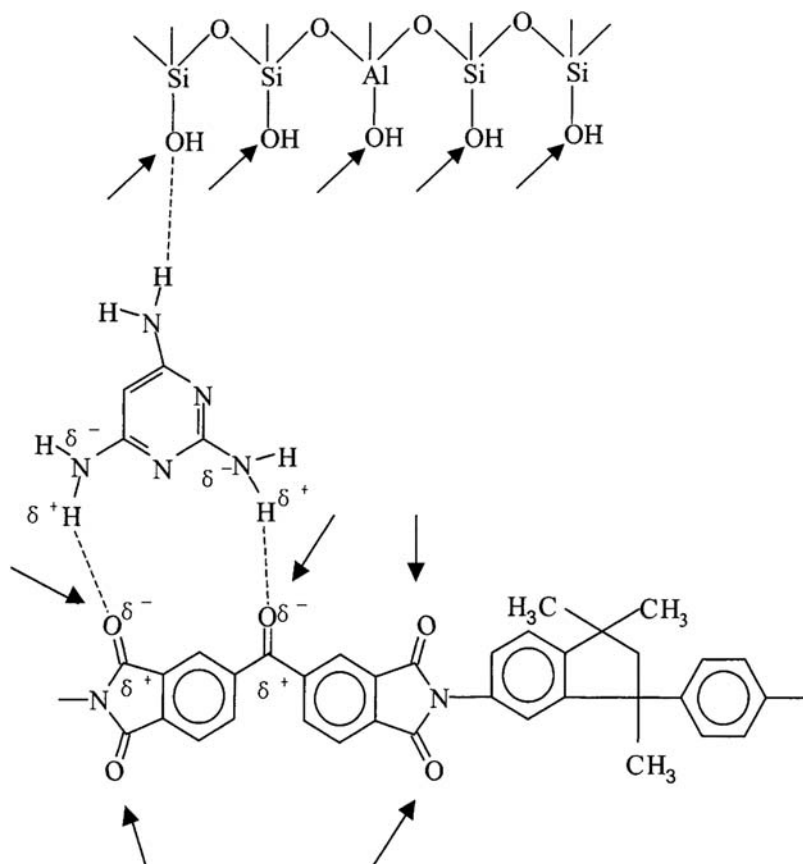


Figure 11.12 The bridging role of 2,4,6-triaminopyrimidine. *Source:* Reprinted with permission from H.H. Yong, H.C. Park, Y.S. Kang, J. Won, W.N. Kim, Zeolite-filled polyimide membrane containing 2,4,6-triaminopyrimidine, *J. Memb. Sci.* 188 (2001) 151–163, Copyright Elsevier.

of zeolite-based nanocomposite membranes in pervaporation are tabulated in [Table 11.2](#). Suhas et al. [34] prepared a PVA mixed matrix membrane containing 7% H-ZSM-5 for pervaporation of water–ethanol and water–IPA mixtures. The zeolite particles had silica by alumina ratios of 38, 187, and 408. They observed that the membrane showed an excellent separation factor of 349 and 568 for water (4%)/ethanol and water (10%)/IPA, respectively, at 30°C feed temperature and 133.3 Pa permeate vacuum pressure. Those separation factors were obtained for membrane with zeolite that contains the highest alumina content. The separation factor was increased with the increase

Table 11.2 Performances of zeolite-based polymer nanocomposite membranes in pervaporation.

Membrane: zeolite (in wt.)/polymer	Feed (in wt.%)	T (°C); P_{permeate} (Pa)	Separation factor (—)	Flux (g m⁻² h⁻¹)	Reference
NaA (15%)/PBZ	Water (10%)—ethanol	70; 1333	100,000	1071	[92]
NaA (10%)/PAAS	Water (10%)—ethanol	30; 135	313.2	440.8	[93]
APTES-NaA (10%)/PAAS	Water (10%)—ethanol	30; 135	435.7	533.2	[93]
NaA (5%)/PVA	Water—butanol (4%)	25; 340	24.14	1866	[94]
NaA (85%)/PES	Water (10%)—ethanol	75; —	>10,000	11,500	[95]
KA (11%)/PVA	Water (20%)—ethanol	50; 13.3	40	164	[96]
CaA (11%)/PVA	Water (20%)—ethanol	50; 13.3	22.3	194	[96]
Zeolite-13X (20%)/polyimide	Water (20%)—ethanol	35; 66.7	5118 ^a	121	[97]
H-ZSM-5 (7%)/PVA	Water (4%)—ethanol	30; 133.3	349	125	[34]
H-ZSM-5 (7%)/PVA	Water (10%)—IPA	30; 133.3	568	144	[34]
ZSM-5 (5%)/PEBA	Butanol (2.5%)—water	45; 320	30.7	569	[98]
ZSM-5 (30%)/PDMS/PES	Butanol (4.5%)—water	31; 600	30.5	113	[35]
Silane-ZSM-5 (20%)/PDMS	Ethanol (10%)—water	40; —	14.1	348	[99]
Chlorosilane-ZSM-5 (30%)/PDMS	Ethanol (5%)—water	40; 100	15.8	202.9	[100]
Silicalite-1 (30%)/PDMS	Ethanol (4%)—water	25; 200	16.5	200	[36]
Silicalite-1 (65%)/PDMS	Acetone (0.5%)—butanol (1.0%)— ethanol (0.15%)—water	50; —	~50 ^a	~20 ^b	[101]
Silicalite-1 (67%)/PDMS	Ethanol (5%)—water	60; 300	15.5	5520	[102]
Chlorosilane-silicalite-1 (50%)/ PDMS	Ethanol (5%)—water	40; —	19.9	66.3	[103]
VTES-silicalite-1 (60%)/PDMS	Ethanol (5%)—water	50; 170—210	26	230	[104]

APTES, 3-Aminopropyltriethoxysilane; PAAS, poly(acrylic acid) sodium; PBZ, polybenzoxazine; PDMS, polydimethylsiloxane; PEBA, poly(ether-block-amide); PES, polyethersulfone; PVA, poly(vinyl) alcohol.

^aSelectivity.

^bAcetone.

in alumina composition, which was associated with better zeolite–polymer interaction. The effect of Si to Al ratio on the separation properties of ZSM-5/polymer membrane was also examined by Xue and Shi [35]. By increasing Si/Al ratio from 25 to 300, they observed that the separation factor for an *n*-butanol aqueous solution was increased to 24.1 from its initial separation factor of 16.5. Those studies confirmed the tailorable hydrophilic/hydrophobic properties of zeolite that facilitate the improvement of zeolite–polymer membrane separation properties.

Tan et al. [98] prepared and investigated the performance of ZSM-5/PEBA membrane for separation of *n*-butanol from water mixture. They found that 5% ZSM-5 was the optimum zeolite concentration and the higher concentration yielded in zeolite agglomeration. The membrane showed enhancing flux and selectivity with increasing temperature and butanol concentration. As the temperature increased, more rapid adsorption–desorption rate occurred in the membrane phase. According to the activation energy analysis, they found that the transport of butanol was much more temperature-sensitive than the water. It explained why the *n*-butanol permeated across the membrane faster than water when the operating temperature was shifted. The higher flux at the higher temperature was also associated with the increasing motion of the polymer segment of the PEBA matrix. Therefore, the enhanced flux at higher temperature was observed both in PEBA and ZSM-5/PEBA membranes. Even though water and *n*-butanol have a smaller size than the pore of zeolite channels, the preferential sorption induces selective separation. The selective *n*-butanol transport can be due to the formation of preferential pathway created by zeolite in the membrane matrix, causing water to permeate through the polymer phase more than through the zeolite channels [32].

Silicalite-1/PDMS membrane was prepared by Yadav et al. [36] for pervaporation of ethanol in the water mixture. The membrane showed increasing separation properties, both in flux and separation factor, with the increase in zeolite loading (from 0% to 30%). Nanocomposite membrane with 30% silicalite-1 content could achieve 16.5 separation factor for ethanol (4%)–water solution, which was higher than those in pure PDMS membrane (8.0). The interesting feature of the zeolite-filled polymeric membrane is the enhanced separation factor. By introducing more zeolite content, an excellent selectivity can be achieved. A relatively high zeolite content, up to 67%, has

been used in silicalite-1/PDMS membrane [102]. Improving membrane separation properties as the effect of increasing zeolite loading was also observed in the gas separation membrane [105]. It should be noted that too high zeolite loading may affect the membrane mechanical strength. Also high particles content may lead to selectivity loss due to the formation of more voids in the interface between polymer and particles [8].

Zeolite–polymer compatibility is one of important factors determining the separation properties of zeolite-based polymer nanocomposite membrane. To improve LTA zeolite-poly(acrylic acid) sodium compatibility, Wei et al. [93] modified LTA zeolite crystal with APTES. The reaction between LTA and APTES yielded in the surface-modified LTA crystal. They found that modified LTA/PAAS membrane exhibited better separation properties than unmodified LTA/PAAS membrane. Modification of LTA crystal resulted in better dispersion and more homogeneous structure. On the other hand, the introduction of unmodified LTA crystal produced a membrane with more voids as the results of zeolite–polymer incompatibility.

Excellent performance of zeolite/polymer membrane was demonstrated by Chuntanaler et al. [92] in the dehydration process. They synthesized NaA-filled polybenzoxaine (PBZ) membrane for ethanol dehydration. The incorporation of 15% zeolite significantly improved the separation factor from 10,000 to >100,000 and flux from ~ 25 to $1071 \text{ g m}^{-2} \text{ h}^{-1}$. This study confirmed the attractive combination of zeolite and polymer.

Another important operating condition in pervaporation is feed composition. For instance, Gu et al. [106] prepared silicalite-filled PEBA for removing ethanol from an aqueous solution. PEBA membrane with 2% silicalite showed an increasing separation factor from ~ 3 to ~ 4 when ethanol concentration was increased from 2% to 10% at 40°C . Since silicalite zeolite is hydrophobic, ethanol flux is higher than water. Also, the increasing ethanol concentration would provide a more driving force for ethanol transport. As a result, the separation factor was increased.

It was demonstrated by several studies that incorporating nanoparticles zeolite into a polymer matrix can successfully improve the separation properties of polymeric membrane. However, one should note that membrane separation properties also depend on zeolite–polymer compatibility. Therefore the method of the preparation of defect-free zeolite/polymer by improving zeolite–polymer compatibility is the crucial factor for obtaining high separation performance.

11.7 Conclusions

As the key factor of process efficiency, the development of highly permeable and selective membranes is crucial for industrial application of pervaporation. Even though polymeric membranes have been widely used, they still have some limitations such as the trade-off between permeability and selectivity as well as low durability against harsh conditions. The incorporation of nanoparticles into the polymeric membrane matrix has been considered as an effective way for improving the separation properties of the polymeric membrane. Zeolites are among the interesting materials for this purpose because they have well-defined structures which allow obtaining nanocomposite membrane with high separation factor. The tailorable hydrophilic–hydrophobic characteristic also allows one to improve the selective sorption of zeolite toward the permeated component so the zeolite-filled membrane can attain higher selectivity.

The separation performance of zeolite-filled nanocomposite membranes or MMMs is determined by the presence of zeolite particles, polymer matrices, and interaction between zeolite and polymer. The separation mechanism inside the membranes will combine the separation mechanism of pure zeolite and pure polymeric materials. The separation of components through zeolite particles can be elucidated by the adsorption of selected component(s) into the pores of zeolites and the diffusion of components along the surface of zeolite mechanisms. In addition to the adsorption and diffusion mechanisms, the separation can also be described by the molecular sieving mechanism. The difference in molecular size between water and alcohol could potentially be exploited by finding suitable zeolite with suitable pore size. The extent of the separation through the pervaporation membrane can be controlled by controlling the chemical potential gradient, which acts as the driving force for separation. The separation mechanism in pervaporation is mainly described by the solution-diffusion model. However, in some cases, the pore-flow model is also used to explain the separation mechanism.

The effect of zeolite addition into polymer matrix on pervaporation membrane performance has been examined in numerous studies. It was reported that the incorporation of zeolite nanoparticles into polymer matrix could successfully improve the separation of organic–aqueous solutions. The separation performance increases with the increasing zeolite loading. However, too high zeolite loading may lead to the selectivity loss due to the formation of more free volume at the interface between zeolite and polymer matrix.

Despite the excellent performance of the zeolite-filled membrane, fabricating defect-free zeolite-based nanocomposite membrane is quite challenging due to the poor zeolite–polymer compatibility and dispersibility. Several strategies to improve zeolite–polymer compatibility have been proposed, such as by employing inorganic or organic bridging agents, priming method, and annealing. By using those strategies, better zeolite–polymer compatibility, as well as improved membrane separation properties, can be obtained.

References

- [1] H.-X. Liu, N. Wang, C. Zhao, S. Ji, J.-R. Li, Membrane materials in the pervaporation separation of aromatic/aliphatic hydrocarbon mixtures—a review, *Chin. J. Chem. Eng.* 26 (2018) 137–143. Available from: <https://doi.org/10.1016/j.cjche.2017.03.006>.
- [2] Z. Xie, N. Li, Q. Wang, B. Bolto, 6 - Desalination by pervaporation, in: V.G.B. T.-E.T. for S.D.H. Gude (Ed.), Butterworth-Heinemann, 2018, pp. 205–226. <https://doi.org/10.1016/B978-0-12-815818-0.00006-0>.
- [3] D. Mangindaan, K. Khoiruddin, I.G. Wenten, Beverage dealcoholization processes: past, present, and future, *Trends Food Sci. Technol.* 71 (2018) 36–45. Available from: <https://doi.org/10.1016/j.tifs.2017.10.018>.
- [4] M. Purwasasmita, D. Kurnia, F.C. Mandias, K. Khoiruddin, I.G. Wenten, Beer dealcoholization using non-porous membrane distillation, *Food Bioprod. Process.* 94 (2015) 180–186. Available from: <https://doi.org/10.1016/j.fbp.2015.03.001>.
- [5] I.G. Wenten, K. Khoiruddin, P.T.P. Aryanti, A.N. Hakim, Scale-up strategies for membrane-based desalination processes: a review, *J. Membr. Sci. Res.* 2 (2016) 42–58. Available from: <https://doi.org/10.22079/JMSR.2016.19152>.
- [6] J. Meng, P. Li, B. Cao, High-flux direct-contact pervaporation membranes for desalination, *ACS Appl. Mater. Interfaces* (2019). Available from: <https://doi.org/10.1021/acsami.9b08078>.
- [7] Y. long Xue, C.H. Lau, B. Cao, P. Li, Elucidating the impact of polymer crosslinking and fixed carrier on enhanced water transport during desalination using pervaporation membranes, *J. Memb. Sci.* 575 (2019) 135–146. Available from: <https://doi.org/10.1016/j.memsci.2019.01.012>.
- [8] R. Castro-Muñoz, G. Francesco, F. Vlastimil, D. Enrico, F. Alberto, Mixed matrix membranes (MMMs) for ethanol purification through pervaporation: current state of the art, *Rev. Chem. Eng.* 0 (2018). Available from: <https://doi.org/10.1515/revce-2017-0115>.
- [9] F.M. Gunawan, D. Mangindaan, K. Khoiruddin, I.G. Wenten, Nanofiltration membrane cross-linked by m-phenylenediamine for dye removal from textile wastewater, *Polym. Adv. Technol.* 30 (2019) 360–367. Available from: <https://doi.org/10.1002/pat.4473>.
- [10] G. Yang, Z. Xie, M. Cran, D. Ng, S. Gray, Enhanced desalination performance of poly (vinyl alcohol)/carbon nanotube composite pervaporation membranes via interfacial engineering, *J. Memb. Sci.* 579 (2019) 40–51. Available from: <https://doi.org/10.1016/j.memsci.2019.02.034>.

- [11] L.M. Robeson, The upper bound revisited, *J. Memb. Sci.* 320 (2008) 390–400. Available from: <https://doi.org/10.1016/j.memsci.2008.04.030>.
- [12] U.W.R. Siagian, A. Raksajati, N.F. Himma, K. Khoiruddin, I.G. Wenten, Membrane-based carbon capture technologies: membrane gas separation vs. membrane contactor, *J. Nat. Gas. Sci. Eng.* 67 (2019) 172–195. Available from: <https://doi.org/10.1016/j.jngse.2019.04.008>.
- [13] N.F. Himma, A.K. Wardani, N. Prasetya, P.T.P. Aryanti, I.G. Wenten, Recent progress and challenges in membrane-based O₂/N₂ separation, *Rev. Chem. Eng.* 35 (2019) 591–626. Available from: <https://doi.org/10.1515/revce-2017-0094>.
- [14] X. Cheng, F. Pan, M. Wang, W. Li, Y. Song, G. Liu, et al., Hybrid membranes for pervaporation separations, *J. Memb. Sci.* 541 (2017) 329–346. Available from: <https://doi.org/10.1016/j.memsci.2017.07.009>.
- [15] H. Julian, P.D. Sutrisna, A.N. Hakim, H.O. Harsono, Y.A. Hugo, I.G. Wenten, Nano-silica/polysulfone asymmetric mixed-matrix membranes (MMMs) with high CO₂ permeance in the application of CO₂/N₂ separation, *Polym. Technol. Mater.* 58 (2019) 678–689. Available from: <https://doi.org/10.1080/03602559.2018.1520253>.
- [16] K. Ueno, H. Negishi, M. Miyamoto, S. Uemiya, Y. Oumi, Effect of Si/Al ratio and amount of deposited MFI-type seed crystals on the separation performance of silicalite-1 membranes for ethanol/water mixtures in the presence of succinic acid, *Microporous Mesoporous Mater.* 267 (2018) 1–8. Available from: <https://doi.org/10.1016/j.micromeso.2018.03.005>.
- [17] I.G. Wenten, P.T. Dharmawijaya, P.T.P. Aryanti, R.R. Mukti, K. Khoiruddin, LTA zeolite membranes: current progress and challenges in pervaporation, *RSC Adv.* 7 (2017) 29520–29539. Available from: <https://doi.org/10.1039/C7RA03341A>.
- [18] T.C. Bowen, R.D. Noble, J.L. Falconer, Fundamentals and applications of pervaporation through zeolite membranes, *J. Memb. Sci.* 245 (2004) 1–33. Available from: <https://doi.org/10.1016/j.memsci.2004.06.059>.
- [19] L.M. Vane, Review: membrane materials for the removal of water from industrial solvents by pervaporation and vapor permeation, *J. Chem. Technol. Biotechnol.* 94 (2019) 343–365. Available from: <https://doi.org/10.1002/jctb.5839>.
- [20] Y. Li, H. Zhou, G. Zhu, J. Liu, W. Yang, Hydrothermal stability of LTA zeolite membranes in pervaporation, *J. Memb. Sci.* 297 (2007) 10–15. Available from: <https://doi.org/10.1016/j.memsci.2007.03.041>.
- [21] Y. Hasegawa, T. Nagase, Y. Kiyozumi, T. Hanaoka, F. Mizukami, Influence of acid on the permeation properties of NaA-type zeolite membranes, *J. Memb. Sci.* 349 (2010) 189–194. Available from: <https://doi.org/10.1016/j.memsci.2009.11.052>.
- [22] C. Yu, Y. Liu, G. Chen, X. Gu, W. Xing, Pretreatment of isopropanol solution from pharmaceutical industry and pervaporation dehydration by NaA zeolite membranes, *Chin. J. Chem. Eng.* 19 (2011) 904–910. Available from: [https://doi.org/10.1016/S1004-9541\(11\)60071-2](https://doi.org/10.1016/S1004-9541(11)60071-2).
- [23] R. Wang, N. Ma, Y. Yan, Z. Wang, Ultrasonic-assisted fabrication of high flux T-type zeolite membranes on alumina hollow fibers, *J. Memb. Sci.* 548 (2018) 676–684. Available from: <https://doi.org/10.1016/j.memsci.2017.10.047>.
- [24] X. Wang, J. Jiang, D. Liu, Y. Xue, C. Zhang, X. Gu, Evaluation of hollow fiber T-type zeolite membrane modules for ethanol dehydration, *Chin. J. Chem. Eng.* 25 (2017) 581–586. Available from: <https://doi.org/10.1016/j.cjche.2016.10.025>.

- [25] X. Chen, J. Wang, D. Yin, J. Yang, J. Lu, Y. Zhang, et al., High-performance zeolite T membrane for dehydration of organics by a new varying temperature hot-dip coating method, *AIChE J.* 59 (2013) 936–947.
- [26] M. Kondo, H. Kita, Permeation mechanism through zeolite NaA and T-type membranes for practical dehydration of organic solvents, *J. Memb. Sci.* 361 (2010) 223–231. Available from: <https://doi.org/10.1016/j.memsci.2010.05.048>.
- [27] Y. Hasegawa, C. Abe, M. Nishioka, K. Sato, T. Nagase, T. Hanaoka, Formation of high flux CHA-type zeolite membranes and their application to the dehydration of alcohol solutions, *J. Memb. Sci.* 364 (2010) 318–324. Available from: <https://doi.org/10.1016/j.memsci.2010.08.022>.
- [28] M. Sugita, T. Takewaki, K. Oshima, N. Fujita, Inorganic Porous Support-Zeolite Membrane Composite, Production Method Thereof, and Separation Method Using the Composite, US Patent No. 8,376,148, 2013.
- [29] Y. Zhang, S. Chen, R. Shi, P. Du, X. Qiu, X. Gu, Pervaporation dehydration of acetic acid through hollow fiber supported DD3R zeolite membrane, *Sep. Purif. Technol.* 204 (2018) 234–242. Available from: <https://doi.org/10.1016/j.seppur.2018.04.066>.
- [30] J. Kuhn, K. Yajima, T. Tomita, J. Gross, F. Kapteijn, Dehydration performance of a hydrophobic DD3R zeolite membrane, *J. Memb. Sci.* 321 (2008) 344–349. Available from: <https://doi.org/10.1016/j.memsci.2008.05.008>.
- [31] X. Zhan, J. Lu, T. Tan, J. Li, Mixed matrix membranes with HF acid etched ZSM-5 for ethanol/water separation: preparation and pervaporation performance, *Appl. Surf. Sci.* 259 (2012) 547–556. Available from: <https://doi.org/10.1016/j.apsusc.2012.05.167>.
- [32] L.M. Vane, V.V. Namboodiri, T.C. Bowen, Hydrophobic zeolite-silicone rubber mixed matrix membranes for ethanol-water separation: effect of zeolite and silicone component selection on pervaporation performance, *J. Memb. Sci.* 308 (2008) 230–241. Available from: <https://doi.org/10.1016/j.memsci.2007.10.003>.
- [33] S. Mosleh, T. Khosravi, O. Bakhtiari, T. Mohammadi, Zeolite filled polyimide membranes for dehydration of isopropanol through pervaporation process, *Chem. Eng. Res. Des.* 90 (2012) 433–441. Available from: <https://doi.org/10.1016/j.cherd.2011.07.021>.
- [34] D.P. Suhas, T.M. Aminabhavi, A.V. Raghu, Mixed matrix membranes of H-ZSM5-loaded poly(vinyl alcohol) used in pervaporation dehydration of alcohols: influence of silica/alumina ratio, *Polym. Eng. Sci.* 54 (2014) 1774–1782. Available from: <https://doi.org/10.1002/pen.23717>.
- [35] G. Xue, B. Shi, Performance of various Si/Al ratios of ZSM-5-filled polydimethylsiloxane/polyethersulfone membrane in butanol recovery by pervaporation, *Adv. Polym. Technol.* 37 (2018) 3095–3105. Available from: <https://doi.org/10.1002/adv.22080>.
- [36] A. Yadav, M.L. Lind, X. Ma, Y.S. Lin, Nanocomposite silicalite-1/polydimethylsiloxane membranes for pervaporation of ethanol from dilute aqueous solutions, *Ind. Eng. Chem. Res.* 52 (2013) 5207–5212. Available from: <https://doi.org/10.1021/ie303240f>.
- [37] J. Kärger, D.M. Ruthven, *Diffusion in Zeolites and Other Microporous Solids*, John Wiley & Sons, Ltd, New York, 1992.
- [38] A. Abdelrasoul, H. Zhang, C.-H. Cheng, H. Doan, Applications of molecular simulations for separation and adsorption in zeolites, *Microporous Mesoporous Mater.* 242 (2017) 294–348. Available from: <https://doi.org/10.1016/j.micromeso.2017.01.038>.

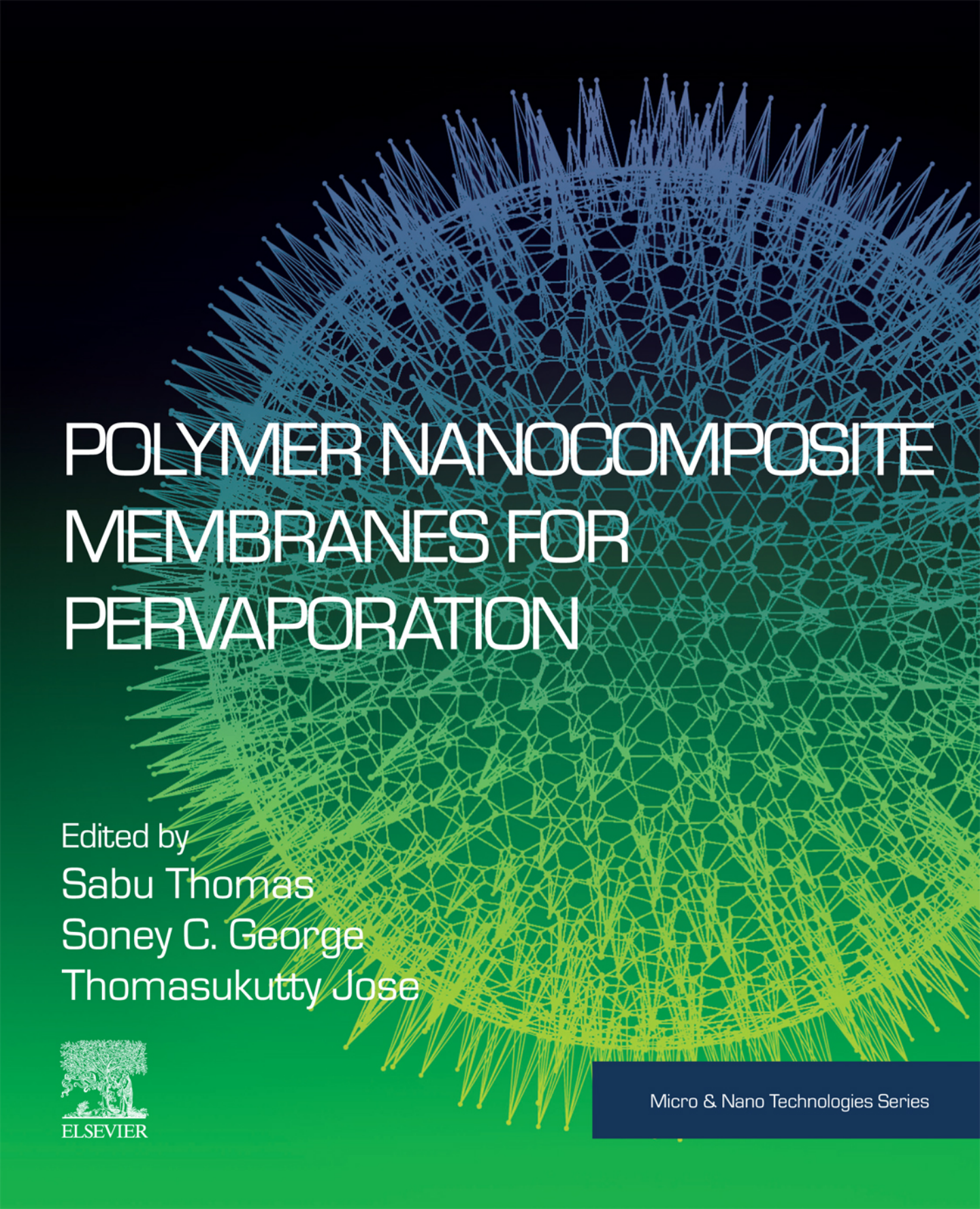
- [39] C. Zhang, L. Peng, J. Jiang, X. Gu, Mass transfer model, preparation and applications of zeolite membranes for pervaporation dehydration: a review, *Chin. J. Chem. Eng.* 25 (2017) 1627–1638. Available from: <https://doi.org/10.1016/j.cjche.2017.09.014>.
- [40] S.C. George, S. Thomas, Transport phenomena through polymeric systems, *Prog. Polym. Sci.* 26 (2001) 985–1017. Available from: [https://doi.org/10.1016/S0079-6700\(00\)00036-8](https://doi.org/10.1016/S0079-6700(00)00036-8).
- [41] N. Kosinov, J. Gascon, F. Kapteijn, E.J.M. Hensen, Recent developments in zeolite membranes for gas separation, *J. Memb. Sci.* 499 (2016) 65–79. Available from: <https://doi.org/10.1016/j.memsci.2015.10.049>.
- [42] Y.K. Ong, G.M. Shi, N.L. Le, Y.P. Tang, J. Zuo, S.P. Nunes, et al., Recent membrane development for pervaporation processes, *Prog. Polym. Sci.* 57 (2016) 1–31. Available from: <https://doi.org/10.1016/j.progpolymsci.2016.02.003>.
- [43] Z. Jia, G. Wu, Metal-organic frameworks based mixed matrix membranes for pervaporation, *Microporous Mesoporous Mater.* 235 (2016) 151–159. Available from: <https://doi.org/10.1016/j.micromeso.2016.08.008>.
- [44] B. Van der Bruggen, P. Luis, Pervaporation as a tool in chemical engineering: a new era? *Curr. Opin. Chem. Eng.* 4 (2014) 47–53.
- [45] B. Smitha, D. Suhanya, S. Sridhar, M. Ramakrishna, Separation of organic–organic mixtures by pervaporation—a review, *J. Memb. Sci.* 241 (2004) 1–21. Available from: <https://doi.org/10.1016/j.memsci.2004.03.042>.
- [46] L. Li, Development of Pervaporation Composite Membranes for Brine Desalination Application, The University of New South Wales (UNSW), 2018. internal-pdf://215.155.228.241/public_version-linli.pdf.
- [47] T. Okada, M. Yoshikawa, T. Matsuura, A study on the pervaporation of ethanol/water mixtures on the basis of pore flow model, *J. Memb. Sci.* 59 (1991) 151–168. Available from: [https://doi.org/10.1016/S0376-7388\(00\)81180-1](https://doi.org/10.1016/S0376-7388(00)81180-1).
- [48] J.G. Wijmans, R.W. Baker, The solution-diffusion model: a review, *J. Memb. Sci.* 107 (1995) 1–21. Available from: [https://doi.org/10.1016/0376-7388\(95\)00102-I](https://doi.org/10.1016/0376-7388(95)00102-I).
- [49] R.W. Baker, J.G. Wijmans, Y. Huang, Permeability, permeance and selectivity: a preferred way of reporting pervaporation performance data, *J. Memb. Sci.* 348 (2010) 346–352. Available from: <https://doi.org/10.1016/j.memsci.2009.11.022>.
- [50] Y. Li, W. Yang, Microwave synthesis of zeolite membranes: A review, *J. Memb. Sci.* 316 (2008) 3–17. Available from: <https://doi.org/10.1016/j.memsci.2007.08.054>.
- [51] P. Luis, B. Van der Bruggen, 4 - Pervaporation modeling: state of the art and future trends, in: A. Basile, M.B.T.-P. Figoli (Eds.), *Khayet Vapour Permeation and Membrane Distillation*, Woodhead Publ. Ser. Energy, Woodhead Publishing, Oxford, 2015, pp. 87–106. Available from: <https://doi.org/10.1016/B978-1-78242-246-4.00004-0>.
- [52] T.-S. Chung, L.Y. Jiang, Y. Li, S. Kulprathipanja, Mixed matrix membranes (MMMs) comprising organic polymers with dispersed inorganic fillers for gas separation, *Prog. Polym. Sci.* 32 (2007) 483–507. Available from: <https://doi.org/10.1016/j.progpolymsci.2007.01.008>.
- [53] T.T. Moore, W.J. Koros, Non-ideal effects in organic–inorganic materials for gas separation membranes, *J. Mol. Struct.* 739 (2005) 87–98. Available from: <https://doi.org/10.1016/j.molstruc.2004.05.043>.

- [54] M.A. Aroon, A.F. Ismail, T. Matsuura, M.M. Montazer-Rahmati, Performance studies of mixed matrix membranes for gas separation: a review, *Sep. Purif. Technol.* 75 (2010) 229–242. Available from: <https://doi.org/10.1016/j.seppur.2010.08.023>.
- [55] A.V. Penkova, D. Roizard, Potential interests of carbon nanoparticles for pervaporation polymeric membranes, *Nanostruct. Polym. Membr.* (2016). Available from: <https://doi.org/10.1002/9781118831823.ch11>.
- [56] M.E. Lydon, K.A. Unocic, T.-H. Bae, C.W. Jones, S. Nair, Structure–property relationships of inorganically surface-modified zeolite molecular sieves for nanocomposite membrane fabrication, *J. Phys. Chem. C* 116 (2012) 9636–9645. Available from: <https://doi.org/10.1021/jp301497d>.
- [57] M. Sianipar, S.H. Kim, K. Khoiruddin, F. Iskandar, I.G. Wenten, Functionalized carbon nanotube (CNT) membrane: progress and challenges, *RSC Adv.* 7 (2017) 51175–51198. Available from: <https://doi.org/10.1039/C7RA08570B>.
- [58] P.T.P. Aryanti, M. Sianipar, M. Zunita, I.G. Wenten, Modified membrane with antibacterial properties, *Membr. Water Treat.* 8 (2017) 463–481. Available from: <https://doi.org/10.12989/mwt.2017.8.5.463>.
- [59] N.F. Himma, N. Prasetya, S. Anisah, I.G. Wenten, Superhydrophobic membrane: progress in preparation and its separation properties, *Rev. Chem. Eng.* 35 (2019) 211–238. Available from: <https://doi.org/10.1515/revce-2017-0030>.
- [60] A.K. Wardani, D. Ariono, S. Subagjo, I.G. Wenten, Hydrophilic modification of polypropylene ultrafiltration membrane by air-assisted polydopamine coating, *Polym. Adv. Technol.* 30 (2019) 1148–1155. Available from: <https://doi.org/10.1002/pat.4549>.
- [61] Y. Kang, L. Emdadi, M.J. Lee, D. Liu, B. Mi, Layer-by-layer assembly of zeolite/polyelectrolyte nanocomposite membranes with high zeolite loading, *Environ. Sci. Technol. Lett.* 1 (2014) 504–509. Available from: <https://doi.org/10.1021/ez500335q>.
- [62] H.-M. Guan, T.-S. Chung, Z. Huang, M.L. Chng, S. Kulprathipanja, Poly (vinyl alcohol) multilayer mixed matrix membranes for the dehydration of ethanol–water mixture, *J. Memb. Sci.* 268 (2006) 113–122. Available from: <https://doi.org/10.1016/j.memsci.2005.05.032>.
- [63] S.S. Madaeni, S. Amirinejad, M. Amirinejad, S.M. Hosseini, A. Khodabakhshi, Cation exchange characterizations of phosphotungstic acid-doped polyvinyl alcohol/polyethersulfone blend membranes by sodium chloride solution, *J. Polym. Eng.* 33 (2013) 71–76.
- [64] F. Parvizian, S.M. Hosseini, A.R. Hamidi, S.S. Madaeni, A.R. Moghadassi, Electrochemical characterization of mixed matrix nanocomposite ion exchange membrane modified by ZnO nanoparticles at different electrolyte conditions “pH/concentration”, *J. Taiwan. Inst. Chem. Eng.* 45 (2014) 2878–2887. Available from: <https://doi.org/10.1016/j.jtice.2014.08.017>.
- [65] S.M. Hosseini, Z. Ahmadi, M. Nemati, F. Parvizian, S.S. Madaeni, Electrodialysis heterogeneous ion exchange membranes modified by SiO₂ nanoparticles: fabrication and electrochemical characterization, *Water Sci. Technol.* 73 (2016) 2074–2084.
- [66] D. Ariono, Khoiruddin, S. Subagjo, I.G. Wenten, Heterogeneous structure and its effect on properties and electrochemical behavior of ion-exchange membrane, *Mater. Res. Express.* 4 (2017) 24006. Available from: <https://doi.org/10.1088/2053-1591/aa5cd4>.

- [67] I.G. Wenten, K. Khoiruddin, Recent developments in heterogeneous ion-exchange membrane: preparation, modification, characterization and performance evaluation, *J. Eng. Sci. Technol.* 11 (2016) 916–934.
- [68] Khoiruddin, D. Ariono, S. Subagio, I.G. Wenten, Surface modification of ion-exchange membranes: methods, characteristics, and performance, *J. Appl. Polym. Sci.* 134 (2017) 45540. Available from: <https://doi.org/10.1002/app.45540>.
- [69] J. Ahmad, M.B. Hägg, Effect of zeolite preheat treatment and membrane post heat treatment on the performance of polyvinyl acetate/zeolite 4 A mixed matrix membrane, *Sep. Purif. Technol.* 115 (2013) 163–171. Available from: <https://doi.org/10.1016/j.seppur.2013.04.050>.
- [70] Q. Ge, Z. Wang, Y. Yan, High-performance zeolite NaA membranes on polymer – zeolite composite hollow fiber supports, *J. Am. Chem. Soc.* 131 (2009) 17056–17057. Available from: <https://doi.org/10.1021/ja9082057>.
- [71] M.G. Buonomenna, W. Yave, G. Golemme, Some approaches for high performance polymer based membranes for gas separation: block copolymers, carbon molecular sieves and mixed matrix membranes, *RSC Adv.* 2 (2012) 10745–10773. Available from: <https://doi.org/10.1039/c2ra20748f>.
- [72] G. Dong, H. Li, V. Chen, Challenges and opportunities for mixed-matrix membranes for gas separation, *J. Mater. Chem. A* 1 (2013) 4610–4630. Available from: <https://doi.org/10.1039/C3TA00927K>.
- [73] Y. Li, T.-S. Chung, C. Cao, S. Kulprathipanja, The effects of polymer chain rigidification, zeolite pore size and pore blockage on polyethersulfone (PES)-zeolite A mixed matrix membranes, *J. Memb. Sci.* 260 (2005) 45–55. Available from: <https://doi.org/10.1016/j.memsci.2005.03.019>.
- [74] K. Zarshenas, A. Raisi, A. Aroujalian, Mixed matrix membrane of nano-zeolite NaX/poly (ether-block-amide) for gas separation applications, *J. Memb. Sci.* 510 (2016) 270–283. Available from: <https://doi.org/10.1016/j.memsci.2016.02.059>.
- [75] A. Ghadimi, T. Mohammadi, N. Kasiri, A. Novel, Chemical surface modification for the fabrication of PEBA/SiO₂ nanocomposite membranes to separate CO₂ from syngas and natural gas streams, *Ind. Eng. Chem. Res.* 53 (2014) 17476–17486. Available from: <https://doi.org/10.1021/ie503216p>.
- [76] B. Yu, H. Cong, Z. Li, J. Tang, X.S. Zhao, Pebax-1657 nanocomposite membranes incorporated with nanoparticles/ colloids/carbon nanotubes for CO₂/N₂ and CO₂/H₂ separation, *J. Appl. Polym. Sci.* 130 (2013) 2867–2876. Available from: <https://doi.org/10.1002/app.39500>.
- [77] H. Wu, X. Li, Y. Li, S. Wang, R. Guo, Z. Jiang, et al., Facilitated transport mixed matrix membranes incorporated with amine functionalized MCM-41 for enhanced gas separation properties, *J. Memb. Sci.* 465 (2014) 78–90. Available from: <https://doi.org/10.1016/j.memsci.2014.04.023>.
- [78] J. Ahmad, M.-B. Hägg, Preparation and characterization of polyvinyl acetate/zeolite 4 A mixed matrix membrane for gas separation, *J. Memb. Sci.* 427 (2013) 73–84. Available from: <https://doi.org/10.1016/j.memsci.2012.09.036>.
- [79] Y. Li, H.-M. Guan, T.-S. Chung, S. Kulprathipanja, Effects of novel silane modification of zeolite surface on polymer chain rigidification and partial pore blockage in polyethersulfone (PES)–zeolite A mixed matrix membranes, *J. Memb. Sci.* 275 (2006) 17–28. Available from: <https://doi.org/10.1016/j.memsci.2005.08.015>.

- [80] X. Ding, X. Li, H. Zhao, R. Wang, R. Zhao, H. Li, et al., Partial pore blockage and polymer chain rigidification phenomena in PEO/ZIF-8 mixed matrix membranes synthesized by in situ polymerization, *Chin. J. Chem. Eng.* 26 (2018) 501–508. Available from: <https://doi.org/10.1016/j.cjche.2017.07.017>.
- [81] R. Mahajan, R. Burns, M. Schaeffer, W.J. Koros, Challenges in forming successful mixed matrix membranes with rigid polymeric materials, *J. Appl. Polym. Sci.* 86 (2002) 881–890. Available from: <https://doi.org/10.1002/app.10998>.
- [82] S. Shu, W.J. Husain, A. Koros, General strategy for adhesion enhancement in polymeric composites by formation of nanostructured particle surfaces, *J. Phys. Chem. C.* 111 (2007) 652–657. Available from: <https://doi.org/10.1021/jp065711j>.
- [83] S. Shu, W.J. Husain, A. Koros, Formation of nanostructured zeolite particle surfaces via a Halide/Grignard Route, *Chem. Mater.* 19 (2007) 4000–4006. Available from: <https://doi.org/10.1021/cm070969n>.
- [84] T.-H. Bae, J. Liu, J.S. Lee, W.J. Koros, C.W. Jones, S. Nair, Facile high-yield solvothermal deposition of inorganic nanostructures on zeolite crystals for mixed matrix membrane fabrication, *J. Am. Chem. Soc.* 131 (2009) 14662–14663. Available from: <https://doi.org/10.1021/ja907435c>.
- [85] T.-H. Bae, J. Liu, J.A. Thompson, W.J. Koros, C.W. Jones, S. Nair, Solvothermal deposition and characterization of magnesium hydroxide nanostructures on zeolite crystals, *Microporous Mesoporous Mater.* 139 (2011) 120–129. Available from: <https://doi.org/10.1016/j.micromeso.2010.10.028>.
- [86] T.-H. Bae, *Engineering Nanoporous Materials for Application in Gas Separation Membranes*, Georgia Institute of Technology, 2010.
- [87] A.F. Ismail, T.D. Kusworo, A. Mustafa, Enhanced gas permeation performance of polyethersulfone mixed matrix hollow fiber membranes using novel Dynasylan Ameo silane agent, *J. Memb. Sci.* 319 (2008) 306–312. Available from: <https://doi.org/10.1016/j.memsci.2008.03.067>.
- [88] T.W. Pechar, S. Kim, B. Vaughan, E. Marand, M. Tsapatsis, H.K. Jeong, et al., Fabrication and characterization of polyimide–zeolite L mixed matrix membranes for gas separations, *J. Memb. Sci.* 277 (2006) 195–202. Available from: <https://doi.org/10.1016/J.MEMSCI.2005.10.029>.
- [89] H.H. Yong, H.C. Park, Y.S. Kang, J. Won, W.N. Kim, Zeolite-filled polyimide membrane containing 2, 4, 6-triaminopyrimidine, *J. Memb. Sci.* 188 (2001) 151–163. Available from: [https://doi.org/10.1016/S0376-7388\(00\)00659-1](https://doi.org/10.1016/S0376-7388(00)00659-1).
- [90] A.M.W. Hillock, S.J. Miller, W.J. Koros, Crosslinked mixed matrix membranes for the purification of natural gas: effects of sieve surface modification, *J. Memb. Sci.* 314 (2008) 193–199. Available from: <https://doi.org/10.1016/j.memsci.2008.01.046>.
- [91] A.F. Ismail, R.A. Rahim, W.A.W.A. Rahman, Characterization of polyethersulfone/Matrimid® 5218 miscible blend mixed matrix membranes for O₂/N₂ gas separation, *Sep. Purif. Technol.* 63 (2008) 200–206. Available from: <https://doi.org/10.1016/j.seppur.2008.05.007>.
- [92] P. Chuntanaler, S. Kulprathipanja, T. Chaisuwan, P. Aungkavattana, K. Hemra, S. Wongkasemjit, Performance polybenzoxazine membrane and mixed matrix membrane for ethanol purification via pervaporation applications, *J. Chem. Technol. Biotechnol.* 91 (2016) 1173–1182. Available from: <https://doi.org/10.1002/jctb.4704>.

- [93] P. Wei, X. Qu, H. Dong, L. Zhang, H. Chen, C. Gao, Silane-modified NaA zeolite/PAAS hybrid pervaporation membranes for the dehydration of ethanol, *J. Appl. Polym. Sci.* 128 (2013) 3390–3397. Available from: <https://doi.org/10.1002/app.38555>.
- [94] D. Oh, S. Lee, Y. Lee, Mixed-matrix membrane prepared from crosslinked PVA with NaA zeolite for pervaporative separation of water–butanol mixtures, *Desalin. Water Treat.* 51 (2013) 5362–5370. Available from: <https://doi.org/10.1080/19443994.2013.768810>.
- [95] J. Li, J. Shao, Q. Ge, G. Wang, Z. Wang, Y. Yan, Influences of the zeolite loading and particle size in composite hollow fiber supports on properties of zeolite NaA membranes, *Microporous Mesoporous Mater.* 160 (2012) 10–17. Available from: <https://doi.org/10.1016/j.micromeso.2012.04.039>.
- [96] Z. Gao, Y. Yue, W. Li, Application of zeolite-filled pervaporation membrane, *Zeolites.* 16 (1996) 70–74. Available from: [https://doi.org/10.1016/0144-2449\(95\)00094-1](https://doi.org/10.1016/0144-2449(95)00094-1).
- [97] C.V. Prasad, B. Yeriswamy, H. Sudhakar, P. Sudhakara, M.C.S. Subha, J.I. Song, et al., Preparation and characterization of nanoparticle-filled, mixed-matrix membranes for the pervaporation dehydration of isopropyl alcohol, *J. Appl. Polym. Sci.* 125 (2012) 3351–3360. Available from: <https://doi.org/10.1002/app.35658>.
- [98] H. Tan, Y. Wu, T. Li, Pervaporation of n-butanol aqueous solution through ZSM-5-PEBA composite membranes, *J. Appl. Polym. Sci.* 129 (2013) 105–112. Available from: <https://doi.org/10.1002/app.38704>.
- [99] L. Ji, B. Shi, L. Wang, Pervaporation separation of ethanol/water mixture using modified zeolite filled PDMS membranes, *J. Appl. Polym. Sci.* 132 (2015). Available from: <https://doi.org/10.1002/app.41897>.
- [100] X. Han, X. Zhang, X. Ma, J. Li, Modified ZSM-5/polydimethylsiloxane mixed matrix membranes for ethanol/water separation via pervaporation, *Polym. Compos.* 37 (2016) 1282–1291. Available from: <https://doi.org/10.1002/pc.23294>.
- [101] H. Zhou, Y. Su, X. Chen, Y. Wan, Separation of acetone, butanol and ethanol (ABE) from dilute aqueous solutions by silicalite-1/PDMS hybrid pervaporation membranes, *Sep. Purif. Technol.* 79 (2011) 375–384. Available from: <https://doi.org/10.1016/j.seppur.2011.03.026>.
- [102] H. Zhou, J. Zhang, Y. Wan, W. Jin, Fabrication of high silicalite-1 content filled PDMS thin composite pervaporation membrane for the separation of ethanol from aqueous solutions, *J. Memb. Sci.* 524 (2017) 1–11. Available from: <https://doi.org/10.1016/j.memsci.2016.11.029>.
- [103] X. Zhan, J. Li, C. Fan, X. Han, Pervaporation separation of ethanol/water mixtures with chlorosilane modified silicalite-1/PDMS hybrid membranes, *Chin. J. Polym. Sci.* 28 (2010) 625–635. Available from: <https://doi.org/10.1007/s10118-010-9136-4>.
- [104] S. Yi, Y. Su, Y. Wan, Preparation and characterization of vinyltriethoxysilane (VTES) modified silicalite-1/PDMS hybrid pervaporation membrane and its application in ethanol separation from dilute aqueous solution, *J. Memb. Sci.* 360 (2010) 341–351. Available from: <https://doi.org/10.1016/j.memsci.2010.05.028>.
- [105] M.G. Süer, N. Baç, L. Yilmaz, Gas permeation characteristics of polymer-zeolite mixed matrix membranes, *J. Memb. Sci.* 91 (1994) 77–86. Available from: [https://doi.org/10.1016/0376-7388\(94\)00018-2](https://doi.org/10.1016/0376-7388(94)00018-2).
- [106] J. Gu, X. Shi, Y. Bai, H. Zhang, L. Zhang, H. Huang, Silicalite-filled PEBA membranes for recovering ethanol from aqueous solution by pervaporation, *Chem. Eng. Technol.* 32 (2009) 155–160. Available from: <https://doi.org/10.1002/ceat.200800252>.



POLYMER NANOCOMPOSITE MEMBRANES FOR PERVAPORATION

Edited by
Sabu Thomas
Soney C. George
Thomasukutty Jose



Micro & Nano Technologies Series

**POLYMER
NANOCOMPOSITE
MEMBRANES FOR
PERVAPORATION**

This page intentionally left blank

POLYMER NANOCOMPOSITE MEMBRANES FOR PERVAPORATION

Edited by

SABU THOMAS

International and Inter University Centre for Nanoscience and
Nanotechnology, Mahatma Gandhi University, Kottayam, India

SONEY C. GEORGE

Centre for Nano Science and Technology, Amal Jyothi College of
Engineering, Kanjirapally, India

THOMASUKUTTY JOSE

Department of Basic Sciences, Centre for Nano Science and Technology,
Amal Jyothi College of Engineering, Kanjirapally, India



ELSEVIER

Elsevier
Radarweg 29, PO Box 211, 1000 AE Amsterdam, Netherlands
The Boulevard, Langford Lane, Kidlington, Oxford OX5 1GB, United Kingdom
50 Hampshire Street, 5th Floor, Cambridge, MA 02139, United States

Copyright © 2020 Elsevier Inc. All rights reserved.

No part of this publication may be reproduced or transmitted in any form or by any means, electronic or mechanical, including photocopying, recording, or any information storage and retrieval system, without permission in writing from the publisher. Details on how to seek permission, further information about the Publisher's permissions policies and our arrangements with organizations such as the Copyright Clearance Center and the Copyright Licensing Agency, can be found at our website: www.elsevier.com/permissions.

This book and the individual contributions contained in it are protected under copyright by the Publisher (other than as may be noted herein).

Notices

Knowledge and best practice in this field are constantly changing. As new research and experience broaden our understanding, changes in research methods, professional practices, or medical treatment may become necessary.

Practitioners and researchers must always rely on their own experience and knowledge in evaluating and using any information, methods, compounds, or experiments described herein. In using such information or methods they should be mindful of their own safety and the safety of others, including parties for whom they have a professional responsibility.

To the fullest extent of the law, neither the Publisher nor the authors, contributors, or editors, assume any liability for any injury and/or damage to persons or property as a matter of products liability, negligence or otherwise, or from any use or operation of any methods, products, instructions, or ideas contained in the material herein.

British Library Cataloguing-in-Publication Data

A catalogue record for this book is available from the British Library

Library of Congress Cataloging-in-Publication Data

A catalogue record for this book is available from the Library of Congress

ISBN: 978-0-12-816785-4

For Information on all Elsevier publications
visit our website at <https://www.elsevier.com/books-and-journals>

Publisher: Matthew Deans
Acquisitions Editor: Simon Holt
Editorial Project Manager: Mariana C. Henriques
Production Project Manager: Prasanna Kalyanaraman
Cover Designer: Greg Harris

Typeset by MPS Limited, Chennai, India



CONTENTS

List of contributors.....	xi
Preface	xv
1 Polymer nanocomposite membranes for pervaporation: an introduction	1
<i>Thomasukutty Jose, Soney C. George and Sabu Thomas</i>	
1.1 Introduction	1
1.2 Basic principles of pervaporation	2
1.3 Membranes for pervaporation	6
1.4 Factors affecting the pervaporation	9
1.5 Advantages of separation using pervaporation process	13
1.6 Conclusions	13
References	14
2 Nanocellulose/polymer nanocomposite membranes for pervaporation application	17
<i>Jithin Joy, Neenu George, Cintil Jose Chirayil and Runcy Wilson</i>	
2.1 Introduction	17
2.2 Nanocellulose isolation methods.....	18
2.3 Nanocellulose/polymer nanocomposite membranes for pervaporation application.....	20
2.4 Conclusions	30
References	31
3 Biobased (nanochitin, nanochitosan) polymer nanocomposite membranes and their pervaporation applications.....	35
<i>Geetha Kathiresan and Naveen Rooba Doss M.</i>	
3.1 Introduction	35
3.2 Pervaporation of chitin and chitosan membranes	36
3.3 Chitin membranes.....	37
3.4 Chitosan membranes.....	37
3.5 Conclusion	75
References	77
Further reading	79

4 Pervaporation performance of polymer/clay nanocomposites81*Runcy Wilson and Gejo George*

4.1 Introduction	81
4.2 Pervaporation characteristics	87
4.3 Factors affecting membrane performance	90
4.4 Conclusions	100
References	100

5 Carbon nanotubes-polymer nanocomposite membranes for pervaporation..... 105*Maryam Ahmadzadeh Tofighy and Toraj Mohammadi*

Nomenclature.....	105
5.1 Introduction	106
5.2 Pervaporation	108
5.3 Polymer nanocomposites	112
5.4 Carbon nanotubes.....	113
5.5 PV application of carbon nanotubes-polymer nanocomposite membranes.....	116
5.6 Conclusions	129
References	129

6 Graphene-based polymer nanocomposite membranes for pervaporation..... 135*M.B. Sethu Lakshmi and Bincy Francis*

6.1 Introduction	135
6.2 Graphene	137
6.3 Graphene-based membranes for pervaporation	141
6.4 Conclusions and future aspects	147
References	148

7 Fullerene and nanodiamond-based polymer nanocomposite membranes and their pervaporation performances 153*Neetha John*

7.1 Introduction	153
7.2 Pervaporation	156

7.3 Membranes for pervaporation	158
7.4 Nanodiamond.....	160
7.5 Pervaporation performance of fullerenes-based nanocomposite membranes.....	162
7.6 Membranes modified with fullerenes and derivatives.....	164
7.7 Conclusions	166
References.....	169
8 Polymer nanocomposite membranes for pervaporation desalination process	175
<i>Deepak Roy George, Shalin Tyni, Asha Elizabeth and Abhinav K. Nair</i>	
8.1 Introduction	175
8.2 Synthesis methods of polymer nanocomposite pervaporation membranes.....	177
8.3 Factors affecting the performance of pervaporation desalination membranes	178
8.4 Polymer membranes for pervaporation desalination	179
8.5 Polymer nanocomposite membranes for pervaporation desalination	184
8.6 Conclusion and future aspects.....	195
References.....	197
9 Polymer/polyhedral oligomeric silsesquioxane nanocomposite membranes for pervaporation	201
<i>Valiya Parambath Swapna, Vakkoottil Sivadasan Abhisha and Ranimol Stephen</i>	
9.1 Introduction	201
9.2 Polyhedral oligomeric silsesquioxane.....	205
9.3 Pervaporation performance of polymer/POSS membranes	210
9.4 Factors affecting the pervaporation through polymer membrane.....	214
9.5 Applications of polyhedral oligomeric silsesquioxane-embedded polymeric systems	218
9.6 Challenges and future aspects	220
References.....	221

10 Nanometal and metal oxide-based polymer nanocomposite membranes for pervaporation	231
<i>Samit Kumar Ray, Amritanshu Banerjee, Swastika Choudhury and Debapriya Pyne</i>	
10.1 Introduction	231
10.2 Synthesis of polymer–nanometal nanocomposite	233
10.3 Direct use of nanometal and metal oxides as membrane	239
10.4 Nanometal and metal oxide-based polymer–metal nanocomposites membranes	239
10.5 Conclusions	255
Acknowledgment.....	257
References.....	257
11 Modified zeolite-based polymer nanocomposite membranes for pervaporation	263
<i>I.G. Wenten, K. Khoiruddin, G.T.M. Kadja, Rino R. Mukti and Putu D. Sutrisna</i>	
11.1 Introduction	263
11.2 Water and alcohol-selective zeolites.....	264
11.3 Mechanism of water/alcohol separation in zeolite	266
11.4 Fabrication of zeolite-filled nanocomposite membranes	275
11.5 Zeolite–polymer compatibility.....	279
11.6 Zeolite–polymer membrane performances in pervaporation...	287
11.7 Conclusions	292
References.....	293
12 Pervaporation and pervaporation-assisted esterification processes using nanocomposite membranes	301
<i>Yavuz Salt, Berk Tirnakci and Inci Salt</i>	
12.1 Introduction	301
12.2 Esters and esterification.....	302
12.3 Combined esterification and reaction systems.....	305
12.4 A unique separation process: pervaporation	306
12.5 Pervaporation membrane reactor	310
12.6 Membranes for membrane reactors.....	313
12.7 Nanocomposite membranes	314
12.8 Conclusions and future recommendations	318
References.....	321

13 Polymer/metal-organic frameworks membranes and pervaporation 329*Peiyong Qin, Zhihao Si, Houchao Shan and Di Cai*

13.1 Introduction	329
13.2 Preparation methods.....	331
13.3 Hydrophobic polymer/metal-organic frameworks membranes for organics recovery	335
13.4 Hydrophilic polymer/metal-organic frameworks membrane for organics dehydration	341
13.5 Challenges and perspectives.....	345
13.6 Final remarks	347
Acknowledgment.....	347
References.....	348

14 Computational modeling of pervaporation process.....355*Muhammad Mujiburohman*

14.1 Definition.....	355
14.2 Pervaporation performance.....	356
14.3 Process conditions	357
14.4 Mass transfer in pervaporation	359
14.5 Transport properties in pervaporation	367
14.6 Sorption of pure liquid <i>i</i> in an amorphous polymer	369
14.7 Pervaporation modeling	373
14.8 Predictive model.....	383
14.9 Conclusion	389
References.....	389

15 Hybrid pervaporation process.....393*Thomasukutty Jose, Soney C. George and Sabu Thomas*

15.1 Introduction	393
15.2 Distillation process.....	394
15.3 Hybrid process parameters	394
15.4 Hybrid distillation–pervaporation process	396
15.5 Simulations of hybrid distillation–pervaporation process	403
15.6 Other pervaporation hybrid processes.....	405
15.7 Advantages of hybrid pervaporation process.....	406
15.8 Conclusion	406
References.....	406

Index.....	409
------------	-----

This page intentionally left blank

List of contributors

Vakkoottil Sivadasan Abhisha Department of Chemistry, St. Joseph's College (Autonomous), Devagiri, Calicut, India

Amritanshu Banerjee Department of Polymer Science & Technology, University of Calcutta, Kolkata, India

Di Cai National Energy R&D Center for Biorefinery, Beijing University of Chemical Technology, Beijing, P.R. China

Cintil Jose Chirayil Newman College, Thodupuzha, India

Swastika Choudhury Department of Polymer Science & Technology, University of Calcutta, Kolkata, India

Asha Elizabeth Department of Chemical Engineering, Amal Jyothi College of Engineering, Kottayam, India

Bincy Francis PG Department of Chemistry, St. Thomas College, Ranny, India

Deepak Roy George Department of Chemical Engineering, Amal Jyothi College of Engineering, Kottayam, India

Gejo George School of Pure & Applied Physics, Mahatma Gandhi University, Kottayam, India

Neenu George St. Joseph's College, Moolamattom, India

Soney C. George Centre For Nanoscience and Technology, Amal Jyothi College of Engineering, Kanjirapally, India

Neetha John Central Institute of Plastics Engineering & Technology (CIPET), Institute of Plastics Technology (IPT), Kochi JNM Campus, Udyogamandal, Kochi, India

Thomasukutty Jose Department of Basic Sciences, Centre For Nanoscience and Technology, Amal Jyothi College of Engineering, Kanjirapally, India

Jithin Joy Newman College, Thodupuzha, India

G.T.M. Kadja Research Center for Nanosciences and Nanotechnology, Institut Teknologi Bandung, Bandung, Indonesia; Division of Inorganic and Physical Chemistry, Institut Teknologi Bandung, Bandung, Indonesia; Center for Catalysis and Reaction Engineering, Institut Teknologi Bandung, Bandung, Indonesia

Geetha Kathiresan Nanotechnology Division, Department of Electronics and Communication Engineering, Periyar Maniammai Institute of Science and Technology, Vallam, Thanjavur, India

K. Khoiruddin Department of Chemical Engineering, Institut Teknologi Bandung, Bandung, Indonesia

Toraj Mohammadi Department of Chemical, Petroleum and Gas Engineering, Center of Excellence for Membrane Research and Technology, Iran University of Science and Technology (IUST), Narmak, Tehran, Iran

Muhammad Mujiburohman Department of Chemical Engineering, Muhammadiyah University of Surakarta, Surakarta, Indonesia

Rino R. Mukti Research Center for Nanosciences and Nanotechnology, Institut Teknologi Bandung, Bandung, Indonesia; Division of Inorganic and Physical Chemistry, Institut Teknologi Bandung, Bandung, Indonesia; Center for Catalysis and Reaction Engineering, Institut Teknologi Bandung, Bandung, Indonesia

Abhinav K. Nair Department of Chemical Engineering, Amal Jyothi College of Engineering, Kottayam, India

Naveen Rooba Doss M. Nanotechnology Division, Department of Electronics and Communication Engineering, Periyar Maniammai Institute of Science and Technology, Vallam, Thanjavur, India

Debapriya Pyne Department of Polymer Science & Technology, University of Calcutta, Kolkata, India

Peiyong Qin National Energy R&D Center for Biorefinery, Beijing University of Chemical Technology, Beijing, P.R. China

Samit Kumar Ray Department of Polymer Science & Technology, University of Calcutta, Kolkata, India

Inci Salt Department of Chemical Engineering, Yildiz Technical University, Esenler, Istanbul, Turkey

Yavuz Salt Department of Chemical Engineering, Yildiz Technical University, Esenler, Istanbul, Turkey

M.B. Sethu Lakshmi Research and PG Department of Chemistry, N.S.S. Hindu College, Changanacherry, India

Houchao Shan National Energy R&D Center for Biorefinery, Beijing University of Chemical Technology, Beijing, P.R. China

Zhihao Si National Energy R&D Center for Biorefinery, Beijing University of Chemical Technology, Beijing, P.R. China

Ranimol Stephen Department of Chemistry, St. Joseph's College (Autonomous), Devagiri, Calicut, India

Putu D. Sutrisna Department of Chemical Engineering, University of Surabaya (UBAYA), Surabaya, Indonesia

Valiya Parambath Swapna Department of Chemistry, St. Joseph's College (Autonomous), Devagiri, Calicut, India

Sabu Thomas International and Inter University Centre for Nanoscience and Nanotechnology, Mahatma Gandhi University, Kottayam, India

Berk Tirnakci Department of Chemical Engineering, Yildiz Technical University, Esenler, Istanbul, Turkey

Maryam Ahmadzadeh Tofighy Department of Chemical, Petroleum and Gas Engineering, Center of Excellence for Membrane Research and Technology, Iran University of Science and Technology (IUST), Narmak, Tehran, Iran

Shalin Tyni Department of Chemical Engineering, Amal Jyothi College of Engineering, Kottayam, India

I.G. Wenten Department of Chemical Engineering, Institut Teknologi Bandung, Bandung, Indonesia; Research Center for Nanosciences and Nanotechnology, Institut Teknologi Bandung, Bandung, Indonesia

Runcy Wilson Department of Chemistry, St. Cyrils College, Adoor, India

This page intentionally left blank

Preface

The new era of membrane technology is keen to develop efficient ways to reduce industrial pollution and energy consumption. Pervaporation is one of the most energy-efficient methods to develop sustainable separation and purification systems. Permeation and evaporation combine to get a cost-effective and pollution-free alternative to conventional separation processes such as distillation. Polymer nanocomposite membranes give more viability to these membrane-based separation technologies. The polymer nanocomposite membranes and their application in pervaporation are the prime area of research to develop new energy-efficient and ecofriendly separation and purification strategies. The recent advancement in polymer nanocomposite membranes and the pervaporation process prompted us to summarize the results in a collective way. The book gives detailed insight into different polymer nanocomposite membranes and their role in pervaporation separation processes. It consists of 15 chapters including a brief introduction about the pervaporation process. The first four chapters exclusively deal with the 21st century nanomaterials such as nanocellulose, nanochitin, and nanoclay-based nanocomposite membranes and its pervaporation applications. The pervaporation performance of nanocomposite membranes with different nanoscale allotropes of carbon (graphene, carbon nanotubes, fullerene, and nanodiamond) is well explained in fifth to seventh chapters. Desalination is another significant area of research, and one chapter is for pervaporation-based desalination processes. Nanocomposite membranes with different nanomaterials such as POSS, nanometal and metal oxides, and modified zeolites and their pervaporation performance are explained in subsequent chapters. The chapters based on computational modeling of the pervaporation and hybrid pervaporation processes add attraction to the readers. The chapters provide detailed insights to young researchers and industrialist to know more about different nanocomposite membranes and their pervaporation applications.

The enormous support and help of all the contributors to the book are well appreciated. We gratefully acknowledge the great efforts of all the reviewers who reviewed the chapters in

the agreed time. A very special word of thanks to the editorial team members of Elsevier for their guidance and continuous support in this venture. We indebted to the support, guidance, and motivation of our management and colleagues. We hope that the book gives a wonderful experience to the readers who focused on theoretical and experimental aspects of pervaporation.

Index

Note: Page numbers followed by “*f*” and “*t*” refer to figures and tables, respectively.

A

- Acetone-butanol-ethanol (ABE)
 - fermentation process, 346
 - Acetyl acetone, as chelating agent, 54–55
 - Acetyl sulfate, sulfonating reagent, 183–184
 - Acid catalyzed hydrolysis, 247–248
 - Acid hydrolysis, 19
 - Acid treatment, 117–118
 - A₃C₆₀ phase, 155
 - Adsorption diffusion model, 97–98
 - Adsorption isotherm, 267–268
 - Aerosol OT (AOT), 237
 - Aging factors, 202–203
 - Alginate, 116–117
 - Alginate-iron nanoparticle composite membrane, 246–247
 - Alginate-iron nanoparticle nanocomposite, 244–245
 - Alkaline hydrolysis, 244–245
 - Alkyl quaternary ammonium compounds, 83–84
 - Alumina, 236–237, 247
 - nanoparticle -based PMNC membranes, pervaporation performance of, 247–249
 - nanoalumina as membrane, 247–248
 - silver polymer, 248–249
 - Aluminum-based metal organic framework (Al-MOF) membrane, 75
 - Aluminum nitrate and sodium hydroxide, 67
 - Aluminum oxide (Al₂O₃), 247
 - γ-Aminopropyl-triethoxysilane (APTEOS), 213–214
 - Ammonium hydroxide, 236
 - Amphiphilic phospholipid, 83–84
 - Anionic octa (tetramethylammonium)-POSS (octa-TMA-POSS), 212–213
 - Anionic polysaccharide, 49
 - Aqueous – organic mixtures, 6–7
 - Arc discharge, 113–114, 137, 154
 - AspenPlus, 404
 - Azeotropes, 108
 - separation, 107
 - Azeotropic distillation separation, 107
 - Azeotropic mixture separation, 2, 201, 210–211
 - and organic solvents, 212–214
 - Azetidino-2,4-dino group, 40
- ## B
- Bacterial cellulose/alginate blend membranes, 30
 - Bentonite
 - clay membrane, 91–92, 92*f*
 - concentration in CMC, 188–189
 - Benzene, carcinogenic, 107
 - Benzene/cyclohexane mixtures separation, 127
 - raw and functionalized MWCNTs effect, 127*f*
 - Benzene – monovalent metal (I) coordinate complex, 65–66
 - Benzyl dimethyl amine, 86
 - Binary liquid mixture, 99
 - Biocompatibility, 20, 35–36, 155–156, 189–190
 - Biodegradable matrix, 81
 - Biodegrading, 35–36
 - Biofiber composites, 81
 - Biomass, 18–19
 - Biom mineralization process, 275–276
 - Biorefinery process, 18
 - Biorenewability, 35–36
 - Bisphenol A epoxy, diglycidyl ether of, 86
 - Black soot, 154
 - Blend
 - inorganic-filled polymeric membrane, 275–276, 277*f*
 - membranes
 - phosphomolybdic acid (PMA)-loaded PVA – poly (vinyl pyrrolidone), 213–214
 - of sodium alginate and (hydroxyethyl) cellulose, 29
 - Boehmite membrane, 67–68
 - Boranes, 146
 - Boron trifluoride monoethyl amine, 86
- ## C
- Cage-structured silsesquioxanes, 206
 - Calcination of metal oxide, 237–238
 - Calcium chloride, 244–245
 - Capping molecule, 236
 - Carbon black, 153
 - Carbon nanotubes (CNTs), 107–108, 113–116, 233

- Carbon nanotubes (CNTs)
 (*Continued*)
 covalent functionalization, 116
 functionalization, 114–116, 115*f*
 noncovalent functionalization, 115
 purification and oxidation of, 114–115
 structure, 113*f*
 total flux and separation factor for water, 245*f*
 tubular structure, 114
- Carbon nanotubes-polymer nanocomposite membranes
 carbon nanotubes, 113–116
 FESEM surface images, 118*f*
 inorganic and organic (polymeric) membranes, 106–107
 pervaporation, 108–112
 applications, 107
 organic – organic mixtures, separation, 125–127
 organics from aqueous solutions, recovery, 128–129
 schematic, 109*f*
 separation characteristics, 110–112
 solution-diffusion model, 109–110
 solvents and alcohols, dehydration of, 116–125
 polymer nanocomposites, 112
 porous and nonporous membranes, 106
- Carboxymethylcellulose (CMC) membrane, 188–189
- Carrageenan membrane, 49
- Catalytic membrane reactors (CMR), 310
- Cationic exchange mechanism, 83–84
- Cationic surfactants, 83–84
- Cellulose, 116–117
 acetate membranes, 23–24, 180
 filled with metal oxide particles, 25–26
 fibers, 20
 membrane, 47–48
 polyacrylonitrile membranes, 23–24
 poly(vinyl alcohol) membranes, 21–23
- Cellulose nanocrystals (NCC), 20
- Cellulose-polydimethyl siloxane blends, 20–21
- Ceramic matrix composites, 81
- Ceramic membranes, 156–157, 159–160
- Cetyltrimethyl ammonium bromide (CTAB), 83–84, 205
- C60-filled ethyl cellulose hybrid membranes, 24
- Chabazite (CHA) zeolite, 265
- Characterization, 21
 alginate – iron nanoparticle composite, 246–247
 enrichment factor, 309
 FESEM, 117–118
 graphene membranes, 139–141
 iron polymer-metal nanocomposites membranes, 246–247
 SEM, 59–60
- Chemical affinity, 17–18
- Chemical potential gradient, 88
- Chemical precipitation, 236
- Chemical reduction, 236
- Chemical vapor decomposition (CVD), 113–114
- Chitin
 and chitosan membranes, 36–37
 membranes, 37
- Chitosan-based membranes, 8
- Chitosan-blended PVP membranes, 41
- Chitosan (CS), 6–7, 116–117, 245–246, 329–330
 FGS membranes, 56–57
 and graphene oxide, 186–187, 187*f*
- hybrid membranes, 76*t*
 aluminum-based metal organic framework membrane, 75
 iron oxide/PAN membrane, 73–74
 PVA/Ag membrane, 71–72
 PVA/multiwall carbon nanotube membrane, 70–71
 silica/PAN/PEG membrane, 74–75
 silica/
 polytetrafluoroethylene membrane, 72–73
 sodium alginate/chitosan/multiwall carbon nanotube membrane, 69–70
- macroradicals, 41
- membranes, 37–75
 chemical structure of, 35*f*, 36
 hybrid membranes, 69–75
 inorganic membranes, 52–68
 interlinking, 39–40
 modification routes for, 39*f*
 modified, 38–39
 organic membranes, 39–52
 water molecules, permeation of, 39*f*
- Chitosan (CS)-based composite membranes, 136–137
- Chitosan/inorganic membranes, 68*t*
 boehmite membrane, 67–68
 clay membrane, 52–54
 ferric oxide membrane, 55–56
 functionalized graphene sheets membrane, 56–57
 multiwall carbon nanotube/silver membrane, 65–66
 Mxene membrane, 66–67
 NaY membrane, 57–58
 phosphorylated chitosan membrane, 63

- phosphotungstic acid membrane, 62–63
 reduced graphene oxide (RGO) membrane, 61–62
 silica membrane, 58–59
 sulfonized chitosan membrane, 63–65
 sulfosuccinic acid membrane, 59–60
 titanium dioxide membrane, 54–55
 toluene-2,4-diisocyanate membrane, 60–61
 Chitosan membranes using TEOS and γ -glycidosypropyltrimethoxysilane (CH-TEOS-GPTS), 58–59
 Chitosan/organic membranes, 53*t*
 carrageenan membrane, 49
 cellulose membrane, 47–48
 gelatin membrane, 49–50
 glutaraldehyde membrane, 50–51
 poly(acrylic acid) membrane, 45
 polyaniline membrane, 51–52
 polybenzimidazole membrane, 40
 poly(*n*-vinyl-2-pyrrolidone) membrane, 40–41
 polyvinyl alcohol membrane, 42–44
 polyvinyl sulfate membrane, 45–46
 sodium alginate membrane, 46–47
 Chitosanpoly(acrylic acid) membrane, 45
 Chitosan – polybenzimidazole membrane, 40
 Chromatographic property, membrane material, 384
 Citric acid, crosslinking agent, 125
 Clay
 crystallite by interlayer cations, 82–83
 materials in desalination membranes, 188–189
 membrane, 52–54
 modification, 83–84
 CMC.
 See Carboxymethylcellulose (CMC) membrane
 CMR. *See* Catalytic membrane reactors (CMR)
 CNTs-polydimethylsiloxane (PDMS) nanocomposite membranes, 128
 Colloids, 236–238
 Column, hybrid process parameters
 cost, 395
 height, 395
 Commercial polyimide (Matrimid), 281–282
 Component flux, 4–5
 Composite membranes, 94, 266–267, 314
 isopropanol/water mixtures, 62–63
 membranes structures, 284–285, 314
 mixed matrix membranes and inorganic fillers incorporated, 270–275
 polymer nanoinorganic particles, 162
 polyvinylamine-PVA separating layer, 120–121
 sol – gel synthesis, 154–155
 water/alcohol separation, 267
 Composites, 81
 biofiber, 81
 ceramic matrix, 81
 fiber-reinforced, 81
 membranes, 314
 metal matrix, 81
 nanofiller-dispersed, 98
 polymer matrix, 81
 Computational modeling, pervaporation (PV), 366
 Concentration gradient, 99
 Concentration polarization, 99
 and partition coefficient, 9
 Condenser heat transfer area, hybrid process parameter, 395
 Contact angle, 384
 Contactor type membrane reactors, 311
 Convective flow, 360
 Conventional separation processes, 201
 Corner-capping reactions, 207–208
 Coupling effect, 372
 Covalent functionalization, 116
 carbon nanotubes, 116
 Covalent grafting, 116
 Crosslinked and modified PVC, 17–18
 Cross-linked hybrid membranes, 162
 Cross-linked membrane, 64*f*
 Cross-linked nanocomposites, 208, 209*f*
 Cross-linked PVA/C-MWCNT/MA, 188, 188*f*
 Cross-linked PVA-multiwalled carbon nanotube (MWCNT) nanocomposite membranes, 317–318
 Cross-linkers, 57–58
 Cross-linking agent, 161, 277–278
 Crystallinity, 19, 37–38, 216
 CS-wrapped MWCNTs incorporated sodium alginate (SA) membranes, 121, 122*f*
 CTAB. *See* Cetyltrimethyl ammonium bromide (CTAB)
 Cussler model, 279–281
 CVD. *See* Chemical vapor decomposition (CVD)
 C-whiskers, 153
 Cyclohexane, 65–66
D
 DDR, 265–266
 Dealumination, 264–265
 Dehydrated ethanol, 91
 Dehydrated isopropanol, 91
 Dehydration, 265–266, 291

- Dendrimers, 231–232
Dense polythene films, 2
Desalination
 of brine, 86–87
 technology, 175–176. *See also*
 Pervaporation desalination
 membranes
Desorption, 110, 309, 362–363
Desulfurization, 220
Diamines, 146
1,6-Diamino hexane, 83–84
Dichloroethane, 37
Diffusion, 110, 308–309, 362
 coefficient, 217, 370
 flux, 358
 selectivity, 2–3
Diffusion-dominated separation
 process, 60–61
Diffusivity, 367–368, 370
 determination, 375–377,
 375*t*, 376*t*
Diisocyanates, 57–58
Dimensional stability, 20
Dimethylacetamide, 182
1,4-Dioxane dehydration, 123
Dip-coating, 333–335
Distributor membrane reactors,
 311
Dodecyl trimethyl ammonium
 bromide, 83–84
Doped silica membranes, 7
Double-walled carbon
 nanotubes (DWCNTs),
 113–114
DWCNTs. *See* Double-walled
 carbon nanotubes (DWCNTs)
- E**
EC/C60 hybrid membrane, 24,
 25*f*
Electrical insulator, 154
Electric laser ablation, 113–114
Electron-rich gasoline
 components, 24
Electrostatic force, 82–83
Energy efficiency, 406
Enrichment factor, 5, 357
Esterification, 160
 pervaporation-assisted, 142
 pervaporation-coupling,
 162
 processes using
 nanocomposite
 membranes, 318–320
 combined esterification
 and reaction systems,
 305–306
 esters and, 302–304
 membrane reactors,
 313–314
 nanocomposite
 membranes, 314–318
 pervaporation and
 pervaporation-assisted
 esterification, 315–318
 pervaporation membrane
 reactor, 310–312
 PV-aided applications,
 319–320
 separation process,
 306–310
 mechanism and basic
 characteristics,
 307–310
 and reaction systems,
 combined, 305–306
 application, 306
 by-product water removal,
 305
 membrane processes, 306
 pervaporation system,
 schematic
 representation, 307*f*
 reactive distillation system,
 schematic
 representation, 305, 306*f*
- Esters and esterification,
 302–304
 acid-catalyzed reactions,
 304
 Fischer esterification, 304
 formula, 302*f*
 hydrogen bonds, 302
Ethanediamine-modified ZIF-8
 particles (ZIF-8-NH₂),
 343–344
Ethanol, 7
 dehydration, 108
 polyhedral oligomeric
 silsesquioxane (POSS),
 218–219
 PV, 20–21
 water dehydration, 45–46
 water mixture, 63–65
Ethyl acetate permeance, 98,
 98*f*
Ethyl cellulose (EC)
 hybrid membrane, 24
 membranes, 28–29
 reinforced with natural
 zeolite membranes, 26–28
 reinforced with TiO₂
 membranes, 29–30
Ethylene glycol pervaporation
 dehydration, 142
Ethyl levulinate, 59–60
Evaporation, 235, 306–307
 permeates, 87–88, 88*f*
 solvent, 273
Exfoliated nanocomposites,
 85–86
Extractor type membrane
 reactors, 311
- F**
Feed concentration, PV
 performance, 357–358
Feed pressure, PV performance,
 358
Ferric oxide
 membrane, 55–56
 nanoparticles, 55–56
Fiber-reinforced composites, 81
Fischer esterification, 304
Flexible selective barrier, 86–87
Flory – Huggins
 thermodynamics, 29, 368
 correlation, 363–364
Flux, 4–5
 reduction and NaCl
 concentration, 183
Free volume elements (FVEs),
 215–216
Free volume of polymer matrix,
 366
Freundlich isotherm, 268
Fuel-cell powered vehicle, 155

- Fuels desulfurization, 220
 Fugacity gradient, 88
 Fullerene-derivative
 carboxyfullerene, 162
 Fullerenes, 231–232
 biological activity, 164–165
 buckyball, 154
 cage compounds, 155
 chemical formula, 154–155
 closed hollow cages, 154
 A₃C₆₀ phase, 155
 endohedral compounds, 155
 exohedral compounds, 155
 functionalization, 156
 membranes modified with,
 164–166
 pervaporation (PV), 156–158
 membranes for, 158–160
 schematic representation,
 157*f*
 production, 154
 Fullerenes-based
 nanocomposite membranes
 performance parameters of
 different pervaporation
 systems, 167*t*
 pervaporation performance,
 162–164
 Fullerenols, 164–165
 Fullerols, 164
 Functionalization, 138–139
 amine, 140–141
 carbon nanotubes, 114–116
 covalent, 116
 fullerenes, 156
 sulfonic acid, 63–65
 surface, 145–146
 Functionalized graphene oxide
 membranes, 145–147
 Functionalized graphene sheet
 (FGS)-based chitosan
 membranes, 56–57
Fusarium oxysporum, 238–239
 FVEs. *See* Free volume elements
 (FVEs)
- G**
 Gas permeation unit (gpu), 5
 Gelatin-based chitosan (GE/
 CH) membranes, 49–50
 Gelatin membrane, 49–50
 Generalized Maxwell – Stefan
 (GMS), 365
 GFT-1005, 159
 Glacial acetic acid, 56–57
 Glass metals, 235
 Glass-transition temperature,
 diffusion process, 216
 Glutaraldehyde (GA), 55–58
 membranes, 50–51, 55–56
 water/acetone solution,
 180–181
 Glycidal POSS-copolyimide
 membranes, 220
 GNPs. *See* Graphene nanoplates
 (GNPs)
 GO. *See* Graphene oxide (GO)
 GO/chitosan (GO/CS)
 nanocomposite membranes,
 317
 Gold nanoparticle-based
 polymer, 253
 plasmon pervaporation, 253
 GO-PAH/hPAN, layer-by-layer
 approach membrane
 thickness, 140, 140*f*
 Graft copolymerization, 239
 Grafting ratio, 51–52
 Graphene, 233
 derivatives, 137–139
 FESEM images
 graphene oxide, 138*f*
 prepared graphene, 138*f*
 graphene oxide (GO) pristine,
 136–137
 graphite to oxidized graphite,
 structure variation, 138*f*
 mechanical properties,
 138–139
 membranes
 for pervaporation, 141–147
 synthesis and
 characterization,
 139–141
 quantum hall effect, 138–139
 sheets, 113–114
 structure and properties,
 137–139
 Graphene-based anion
 exchange membrane, 140
 Graphene-based membranes
 for pervaporation, 141–147
 functionalized graphene
 oxide membranes, 145–147
 graphene oxide-based
 membranes, 141–142
 hybrid graphene oxide
 membranes, 144–145
 quantum dot membranes,
 147
 reduced graphene oxide
 membranes, 143–144
 Graphene nanoplates (GNPs),
 186
 Graphene oxide-based
 membranes, 141–142
 Graphene oxide framework
 (GOF), 140
 Graphene oxide (GO), 61–62,
 186
 FESEM images, 138*f*
 flakes functionalized with 3-
 amino-1-propanesulfonic
 acid (GO_{SULF}), 140
 GO/polyimide (PI) fiber
 membrane, 186
 in polyamide layer (PA-GO),
 145
 reduction, 138
 Graphene oxide membranes
 (GOM), 140
 “Green” chemical process,
 329
- H**
 Hexadecyl trimethyl
 ammonium bromide, 83–84
 Hierarchically ordered stainless-
 steel-mesh (HOSSM),
 340–341
 Hollow fiber membrane,
 278–279
 Homogeneous nanofillers
 distribution, 112

- Hybrid graphene oxide membranes, 144–145
 PA-GO/PAN membrane, 145, 145f
 structures, 144f
- Hybrid plastics, 206–207
- Hybrid processes, 393
 advantages, 406
 distillation – pervaporation process, 396–403, 399f
 distillation process, 394, 395f
 hybrid PV – liquid phase adsorption process, 405
 parameters, 394–395
 PV-coupled fermentation process, 405
 PV-coupled laccase treatment, 405
 simulations, 403–405
- Hybrid PV – liquid phase adsorption process, 405
- Hybrid reactive distillation (RD), 394
- Hydrogen bonding, 82–83
 interactions, 210–211
- Hydrophilic and organophilic membranes, 2
- Hydrophilicity, 241–242
- Hydrophilic membranes, 341
- Hydrophilic polymers, 116–117
 MOFs membranes, 337t, 342t
- Hydrophobic cellulose derivative, 20–21
- Hydrophobic – hydrophilic balance, 55–56
- Hydrophobic membranes, 128, 156–157, 159–160
- Hydrophobic MOF-based MMMs, 335–336
- Hydrosilylation reactions, 207–208
- Hydrothermal method, 237
- Hydroxyethyl cellulose (HEC), 29
- I**
- IAST. *See* Ideal adsorbed solution theory (IAST)
- Ideal adsorbed solution theory (IAST), 268–269
- Imidazolium, 83–84
- IMR. *See* Inert membrane reactors (IMR)
- Inert membrane reactors (IMR), 310–311
- Inorganic adsorbent, 57–58
- Inorganic and organic (polymeric) membranes, 106–107
- Inorganic bridging agents, 283–285
- Inorganic membranes, 7, 159, 233, 275–276, 314
- In situ polymerization, polymer nanocomposite pervaporation membranes, 178
- Intercalated nanocomposites, 85–86
- Interfacial thermodynamics, 384
- Intermatrix synthesis technique, 240
- Intramolecular hydrogen bonds, 42–44
- Intrinsic membrane performance, 5
- Inverse gas chromatography method, 372–373
- Ion exchange capacity (IEC), 49–50
- Iron nanoparticle -based polymer, 242–247
- Iron nanoparticle (FeNP), 242–243
- Iron oxide/PAN membrane, 73–74
- Iron polymer-metal, characterization, 246–247
- 4-Isocyanato-40-(3,30-dimethyl-2, 4-dioxo-azetidino) diphenyl methane (IDD), 40
- Isopropanol/water mixture, 60–61
- K**
- Kaolinite, 83–84
- Kinks, nanometal and metal oxides, 232
- Klein paradox, graphene, 138–139
- Knudsen diffusion, 360
- L**
- Lactobacillus* strain, 238–239
- Lampung Natural Zeolite (LNZ) membranes, 26–28, 27f
- Langmuir adsorption isotherm, 268
- Laponite nanoclay into PVA membranes, 189–190
- Laser ablation, 235
- Layer-by-layer assembly method, 275–276
- Lignocellulosic biomass, 19
 recalcitrance, 19
- Linde type A (LTA) zeolite, 264–265
- Liquid-to-vapor phase transition, 1–2
- Lithium chloride solutions, 37
- M**
- Maleic acid (MA), 181
- Maleic alginate cross-linked sodium alginate/chitosan membrane (M-CA/CH), 46–47
- Maleic anhydride, 44, 46–47
- Mass transfer
 coefficient, 99
 in PV, 359–366
 computational model, 366
 Maxwell – Stefan model, 365–366
 modified solution-diffusion model, 363–364
 pore flow model, 359–361
 solution-diffusion model, 361–363
 thermodynamics model, 364–365
 resistance, 28–29, 188

- Mass transport and membranes, 88, 90, 99
- Matrimid – zeolite A membranes, 281–282
- Maxwell – Stefan model, 365–366
- Mean free path, graphene, 138–139
- Mechanical grinding, 234–235
- Melt mixing, 235
- Membrane, 232–233
fouling, 202–203
isothermal processes, 175–176
module cost, 395
permeability, 111
permeation flux, 111
processes fouling, 175–176
reactors
 classification, 311*f*
 membranes for, 313–314
selectivity, 112
separation
 applications, 46–47
 processes, 393
 technology, 108, 159–160
surface effective area, 111
thickness
 pervaporation, 12
 PV performance, 358
type, 358
- Metal matrix composites, 81
- Metal/metal oxide
nanoparticles, synthesis, 234
biological method, 238–239
chemical methods, 236–238
 chemical precipitation, 236
 chemical reduction, 236
 hydrothermal method, 237
 microemulsion technique, 237–238
 sol-gel technique, 236–237
physical method
 evaporation, 235
 laser ablation, 235
 mechanical grinding, 234–235
 melt mixing, 235
 sputtering, 235
- Metal nanocomposites
membranes, 239–254
 alumina nanoparticle -based
 PMNC membranes,
 pervaporation performance
 of, 247–249
 nanoalumina as
 membrane, 247–248
 silver polymer, 248–249
 gold nanoparticle-based
 polymer, 253
 plasmon pervaporation,
 253
 iron nanoparticle -based
 polymer, 242–247
 iron polymer-metal,
 characterization,
 246–247
 pervaporation with iron
 polymer, 243–246
nanoparticles
 in polymer, incorporation,
 240
 to polymer, grafting, 240
pervaporation
 using Ag polymer, 241–242
 using titanium
 nanoparticle-based
 polymer, 249–252
polymer-metal
nanocomposites based on
nano-MgO and ZnO,
253–254
silver nanoparticle-based
polymer, 241
- Metal-organic frameworks (MOFs), 7–8, 329, 330*f*
- Methanol and methyl tert butyl ether (MeOH-MTBE), 40–41
- Methanol – MTBE mixture, 40–41, 45
- Methylene blue removal, 141–142
- Methylethylketone, 7
- Methyl nicotinamide chloride, 146
- Methyl tertbutyl ether (MTBE)/methanol mixtures, 25
- Microporous silica, 7
- Microcomposite
nanocomposites, 85–86
- Microemulsion technique, 237–238, 253–254
- Microfiltration, 106
- Mitsunobu reaction, 304
- Mixed matrix membranes (MMMs), 7–8, 106–107, 188, 253–254, 263–264, 270–275, 314, 329–331
morphologies and typical defects in, 113*f*, 273
for pervaporation
 desalination, 184–190
 PES – zeolite 4A, 287*f*
- Mobility selectivity, 357
- Modified pervaporation process, 377–382
- Modified solution-diffusion model, 363–364
- Modified zeolite-based polymer nanocomposite membranes compatibility, 279–287, 291
performances in
 pervaporation, 287–291, 289*t*
solution-diffusion mechanism, 264
water/alcohol separation in zeolite, mechanism, 266–275
mixed matrix membranes and inorganic fillers, 270–275
zeolite particles, 267–270
water and alcohol-selective zeolites, 264–266
zeolite-filled nanocomposite membranes, fabrication, 275–279
- Modifier, PV membranes, 161
- MOFs-based MMMs, 334*t*
- Molecular sieving, 360
- Molecular weight, diffusion process, 216
- Monomers, hydrophilic and hydrophobic, 17–18
- Monomethyl hydrazine (MMH) liquid propellants, 28–29

- Montmorillonite, 82–84
- Mordenite framework inverted (MFI)-type structure, 266
- Multiwalled carbon nanotubes (MWCNTs), 65–66, 113–114
- MWCNTs-bucky paper (MWCNT-BP) structure, 123–125
- Mxene-based chitosan composite membrane, 66–67
- MXene membranes, 66–67, 191–192
- laminates, 191–192
- nanosheet and mass transport, 192*f*
- N**
- NaA-filled polybenzoxaine (PBZ), 291
- Nadic methyl anhydride, 86
- Nafion-GO_{SULF} membranes, 140
- Nanoalumina as membrane, 247–248
- Nanocellulose, 18
- isolation methods, 18–19
- polymer nanocomposite membranes
- bacterial cellulose/alginate blend membranes, 30
- blend membranes of sodium alginate and (hydroxyethyl) cellulose, 29
- cellulose acetate membrane filled with metal oxide particles, 25–26
- cellulose acetate/polyacrylonitrile membranes, 23–24
- cellulose-polydimethylsiloxane blends, 20–21
- cellulose/poly(vinyl alcohol) membranes, 21–23
- C60-filled ethyl cellulose hybrid membranes, 24
- ethyl cellulose membranes, 26–30
- membrane materials, design and choice of, 17–18
- nanocellulose isolation methods, 18–19
- pervaporation application, 20–30
- Nanoclay
- clay particles, structure, 82–83
- octahedral sheet, 82–83
- organic modification of, 83–84, 84*f*
- silicon-oxygen tetrahedra, 82–83
- Nano-CNT-iron oxide, 244–245
- Nanocomposite membranes for pervaporation, 6–9, 6*f*, 314–318
- advantages, 13
- esterification, 315–318
- factors affecting, 9–12
- concentration polarization and partition coefficient, 9
- membrane thickness, 12
- pressure, 9
- temperature, 10–11
- inorganic membranes, 7
- mixed matrix membranes, 7–8
- polymer membranes, 8–9
- principles, 2–5
- permeability, normalized flux, 4–5
- pore flow model, 3–4
- selectivity, intrinsic membrane properties, 5
- solution-diffusion model, 2–3
- Nanocrystals, 20
- Nanodiamonds, 155–156, 160–161
- applications, 160–161
- biocompatibility, 155–156
- concentration in smoke, 160–161
- cross section, 156*f*
- in hydrophobic membranes, 161
- mass production, 160–161
- Nanofibrous composite membrane, 191
- Nanofiller-dispersed composites, 98
- Nanofillers, 20, 107–108, 112, 141, 144, 148
- Nanofiltration, 106, 143–144, 175–176, 315
- Nanomaterials
- in membrane applications, 315, 318–319
- surface modification and functionalization, 112
- Nanometals, 232
- and metal oxides
- as membrane, 239
- metal nanocomposites membranes, 239–254
- synthesis, 234*f*
- nanocomposite, 233–239
- Nanoparticle-embedded polymer matrix, 217
- Nanoparticles
- in polymer, incorporation, 240
- to polymer, grafting, 240
- Nanoscale cellulosic materials, 19–20
- Nanostructured semiconductor, 232
- Nanotechnology, 153–154, 233, 314
- Nanotitanium oxide, 236–237
- Nanotubes, 231–232. *See also* Carbon nanotubes (CNTs)
- carbon nanotubes (CNTs), 107–108, 113–116
- multiwalled carbon nanotubes (MWCNTs), 65–66, 113–114
- single-walled carbon nanotubes (SWCNTs), 113–114
- NaY membrane, 57–58

- Neutral and charged copolymers, 17–18
- N-methyl-2-pyrrolidone, 37
- N,N-dimethyl acetamide, 37
- N,N-dimethylformamide solvent, 184–185
- Nonbiodegradable matrix, 81
- Noncaged silsesquioxane molecule, 206, 207*f*
- Noncovalent functionalization, carbon nanotubes, 115
- Nonporous membranes, 106
- Non-porous polymeric membranes, 110
- N-o-sulfonic acidbenzyl chitosan (NSABC) hybridmembranes, 63–65
- O**
- Octadecyl trimethyl ammonium bromide (ODTMA), 83–84
- Octa(tetramethylammonium)-POSS (octa-TMA-POSS), 212–213
- OH-group-modified fulleranol, 156
- Oleyl alcohol, organic liquid membranes, 160
- Oly[β -(1,4)-D-glucosamine], 245–246
- One-dimensional (1D) nanomaterials, 81–82
- Organically modified clays, 83–84
- Organically modified montmorillonite, 86
- Organic bridging agents, 286–287
- Organic chemical vapor deposition, 253–254
- Organic functionalities, 83–84
- Organic – inorganic hybrid membranes, 159, 233
- Organic membranes, 159
- Organic mixtures, separation, 219–220
- Organic polymer membranes, 233
- Organics dehydration, 329
- hydrophilic polymer/MOFs membranes for, 341–345, 342*t*
- Organic-selective membranes, 17–18, 109
- Organic solvent nanofiltration (OSN), 20–21
- Organic – water mixtures, 107
- Organometallic molecules, 155
- Organosilanes, 286*f*
- Osmosis, forward, 175–176
- P**
- Palygorskite clay minerals, 83–84
- Para-toluene sulfonic acid-treated clay-filled sodium alginate membranes, 94
- PEBA-acetic acid, 185
- PEBAX membrane, 182
- Pendent type nanocomposites, 208, 209*f*
- Permeability, 4–5, 372–373
- coefficient, 270–271
- determination, 377
- normalized flux, 4–5
- selectivity, 357
- and selectivity, 17–18
- Permeance, 4–5
- Permeate pressure, PV performance, 358
- Permeation flux, 42–44, 59–60, 110–111, 356, 358
- Permeation performance, 10
- Permeation rate, 12, 377–379
- Permselective evaporation, 2
- PERVAP 2201, 159
- PERVAP 1005 (GFT), 159
- Pervaporation, 135–136, 176, 232–233, 329
- advantages, 13
- chitin and chitosan membranes, 36–37
- definition, 355–356
- experimental set-up for, 136*f*
- factors affecting, 9–12
- concentration polarization and partition coefficient, 9
- membrane thickness, 12
- pressure, 9
- temperature, 10–11
- with iron polymer, 243–246
- mass transfer in, 359–366
- computational model, 366
- Maxwell – Stefan model, 365–366
- modified solution-diffusion model, 363–364
- pore flow model, 359–360
- solution-diffusion model, 361–363
- thermodynamics model, 364–365
- membranes, 6–9, 6*f*
- inorganic membranes, 7
- mixed matrix membranes, 7–8
- polymer membranes, 8–9
- mixed matrix membranes (MMMs), 242*f*
- modeling, 373–382
- diffusivity determination, 375–377
- modified pervaporation process, 377–382
- permeability determination, 377
- sorption coefficient determination, 373–374
- performance, 356–357
- enrichment factor, 357
- separation factor, 357
- plasmon, 253
- polymer-metal nanocomposite membranes, 255*t*
- predictive model, 383–389
- chromatographic property, 384
- contact angle, 384
- interfacial thermodynamics, 384
- physicochemical properties-process conditions, 385–389, 386*t*

- Pervaporation (*Continued*)
polarity and solubility parameter, 383–384
principles, 2–5
permeability, normalized flux, 4–5
pore flow model, 3–4
selectivity, intrinsic membrane properties, 5
solution-diffusion model, 2–3
process conditions, 357–359
pure liquid sorption, 369–373
inverse gas chromatography method, 372–373
time-dependence of sorption, 370–371
time-lag experiment, 371
transport properties in, 367–368
using Ag polymer, 241–242
using titanium nanoparticle-based polymer, 249–252
- Pervaporation desalination membranes
factors affecting, 178–179
filler, diffusivity and nature, 178–179
membrane material, selectivity and nature, 178
operating temperature, 179
salt transport suppression, 179
polymer membranes for, 179–184
cellulose acetate membranes, 180
PEBAX membrane, 182
polyacrylonitrile and polyvinyl alcohol-based membranes, 180–181
poly(vinyl alcohol)/polyvinylidene fluoride pervaporation membrane, 181–182
sulfonated poly(styrene-ethylene/ butylenes-styrene) block copolymer membrane, 183–184
tubular pervaporation membrane, 183
polymer nanocomposite membranes, 184–195
chitosan and graphene oxide, schematic of molecular interactions, 187*f*
mixed matrix membranes for pervaporation desalination, 184–190
self-assembled membranes, 190–192
sol – gel synthesized membranes, 192–195
- Pervaporation desalination process, polymer nanocomposite membranes physical blending, 177
schematic representation, 176*f*
self-assembly method, 178
in situ polymerization, 178
sol – gel synthesis, 177
synthesis methods, 177–178
- Pervaporation membrane reactors (PVMRs), 301–302, 310–312
membrane classification and membrane applications, 313*f*
- Pervaporation separation index (PSI), 309–310
- Phosphonium derivatives, 83–84
- Phosphorylated chitosan membrane, 63
- Phosphotungstic acid membrane, 62–63
- Physical blending, polymer nanocomposite pervaporation membranes, 177
- Physicochemical properties-process conditions, 385–389, 386*t*
- Plasmon excitation, 232
- Plasmon pervaporation, 253
- Plasticization, 202–203
effect, 63
- PMDA. *See* Pyromellitic dianhydride (PMDA)
- Polarity and solubility parameter, 383–384
- Polar polymers, 216
- Polyacrylates, 8–9
- Polyacrylic acid (PAA), 45, 241–242
membrane, 45
- Polyacrylonitrile (PAN)
fibers, 153
and polyvinyl alcohol-based membranes, 180–181
- Poly(allylaminehydrochloride)-wrapped MWCNTs (MWCNTs – PAH), 118–119, 119*f*
- Polyaniline membrane, 51–52
- Polybenzimidazole (PBI), 6–7, 329–330
- Polybenzimidazole membrane, 40
- Poly(2,6-dimethyl-1,4-phenylenoxide) (PPO), 162
- Polydimethyl siloxane/polyphenyl sulfone, 97
- Polydimethylsiloxanes (PDMS), 8–9, 156–157, 160, 329–330
hydrophobic membranes, 2
membranes, 6–7
rubber membrane, 241–242
- Polyelectrolytes, 275–276
aggregates, 47–48
complex, 47–48
complex formation, 45
- Polyesters
as inorganic filler and selective top, 120
polyethylenimines, 8–9
- Poly(ether amides), 8–9
- Poly(ether-block-amide) (PEBA), 329–330, 377–379
copolymer, 182
- Polyethersulfone (PES), 120, 278–279

- Polyethylene glycol (PEG)
blocks copolymer, 236
- Poly(ethylene glycol)-POSS
(PEG-POSS), 212–213
- Polyhedral oligomeric
silsesquioxane (POSS), 7–8,
205–210. *See also* Polymer/
POSS membranes,
pervaporation performance
applications, 208–210, 210*f*
challenges and future
aspects, 220–221
as molecular filler, 205–206
nanomaterial, applications,
210*f*
polymer/POSS membranes,
pervaporation
performance, 210–214
azeotropic mixtures and
organic solvents,
separation, 212–214
cross-linking, 218
filler particles, nature,
216–217
free volume effect, 215–216
nature of, 216
penetrants nature, 218
temperature effect, 217
- POSS-based nanocomposites,
types, 209*f*
- POSS-embedded polymeric
systems, 218–220
ethanol, 218–219
fuels desulfurization, 220
organic mixtures,
separation, 219–220
water treatment, 220
- properties, 208
- silsesquioxanes, structures,
207*f*
- sizes and volume details, 206*f*
- synthesis, 206–208
- THF – water azeotropic
mixture, 212–213, 213*t*
- types, 206
- Poly(3-hydroxybutyrate) (PHB),
123
- Polyimides (PIs), 6–7
- Polymer
free volume, 110
membranes, 8–9
nanoclay composites, 85–87
nanoinorganic particles, 162
nanosized inorganic particle-
based composite materials,
163–164
pervaporation membranes,
329–330
- Polymer-based membranes,
37–38
- Polymer/clay nanocomposites,
81–82
membrane performance,
factors affecting, 90–99
concentration polarization,
99
feed composition, 94–96
nanoclay content effect,
91–94
temperature, 96–98
- nanoclay
organic modification of,
83–84, 84*f*
structure of, 82–83
- pervaporation characteristics,
87–90
advantages and
disadvantages, 89*t*
membrane process,
schematic diagram, 88*f*
polymeric membrane-
based process, 87*t*
pore flow mechanism, 90
solution diffusion
mechanism, 89–90
transport mechanism, 88
- polymer nanoclay
composites, 85–87
- Polymer – filler interactions,
203–205
- Polymeric-based hydrophilic
membranes, 2
- Polymeric membranes, 86–87,
87*t*, 106–107, 263–264,
313–314
- Polymeric nanocomposite
membranes (PNCMs),
106–107
high-performance, 112
- Polymerization, 178
- Polymer-layered
nanocomposites, 81–82
- Polymer matrix, 85–86, 129,
239
composites, 81
- Polymer-metal nanocomposites
(PMNCs), 232–234
based on nano-MgO and
ZnO, 253–254
membranes, 255–257
- Polymer/metal-organic
frameworks membranes,
329–331
hydrophilic polymer/metal-
organic frameworks
membrane for organics
dehydration, 341
metal-organic frameworks/
chitosan membranes,
345
metal-organic frameworks/
polybenzimidazole
membranes, 344
metal-organic frameworks/
poly(vinyl alcohol)
membranes, 343–344
- hydrophobic polymer/metal-
organic frameworks
membranes, organic
recovery, 335–341
polydimethylsiloxane/
metal-organic
frameworks membranes,
336–339
poly(ether-block-amide)/
metal-organic
frameworks membranes,
339–340
- PTMPS/metal-organic
frameworks membranes,
340–341
- preparation methods,
331–335
- Polymer nanocomposite
membranes
pervaporation, 108–112
applications, 107

- Polymer nanocomposite membranes (*Continued*)
- organic – organic mixtures, separation, 125–127
 - organics from aqueous solutions, recovery, 128–129
 - schematic, 109*f*
 - separation characteristics, 110–112
 - solution-diffusion model, 109–110
 - solvents and alcohols, dehydration of, 116–125
- pervaporation desalination process
- physical blending, 177
 - schematic representation, 176*f*
 - self-assembly method, 178
 - in situ polymerization, 178
 - sol – gel synthesis, 177
 - synthesis methods, 177–178
- Polymer nanocomposites, 20, 81–82, 112, 208
- star-like, 208, 209*f*
- Polymer–nanometal nanocomposite, synthesis of, 233–239
- Polymer poly(n-vinyl-2-pyrrolidone) (PVP), 40–41
- Polymer/POSS membranes, pervaporation performance, 210–214. *See also* Polyhedral oligomeric silsesquioxane (POSS)
- azeotropic mixtures and organic solvents, separation, 212–214
 - cross-linking, 218
 - filler particles, nature, 216–217
 - free volume effect, 215–216
 - nature of, 216
 - penetrants nature, 218
 - temperature effect, 217
- Poly(2-methacryloyloxy ethyl trimethyl ammonium chloride) (PDMC), 144–145
- Poly(methyl methacrylates) (PMMA), 8–9
- membranes, 127
- Poly(n-vinyl-2-pyrrolidone) membrane, 40–41
- Poly(phenyleneiso-phthalamide), 98
- Poly(phenyltrimethoxysiloxane) (PTMOS), 277–278
- Poly(phthalazinone ether sulfone ketone)-polyethersulfone (PES)/TiO₂ membranes, 318
- Polypropylene glycol, 83–84
- Poly(sodium 4-styrenesulfonate) (PSS)-wrapped MWCNTs (MWCNTs-PSS), 119, 120*f*
- Poly(sodium vinylsulfate) and chitosan (PVS/CH), 45–46
- Polystyrene/montmorillonite nanocomposites, 83–84
- Polysulfone (PS), 120–121
- SiO₂-GO nanohybrid composite membranes, 140
 - substrate, 336–339
- Poly[1-(trimethylsilyl)-1-propyne] (PTMPS), 329–330
- Polyurethane (PU) membranes, 8–9, 127
- Polyvinyl acetate (PVAc), 281–282
- Polyvinyl alcohol-based iron polymer, 243–244
- Poly(vinyl alcohol) (PVA), 2, 116–117, 156–157, 241–242
- Ag membrane, 71–72
 - bentonite clay membrane, 91–92, 92*f*
 - carboxylic MWCNT (C-MWCNT), 188
 - clay nanocomposite membranes, 93*f*
 - cross-linked with PMDA, 180
 - membrane, 42–44
 - multiwall carbon nanotube membrane, 70–71
 - polyvinylidene fluoride pervaporation membrane, 181–182
- Polyvinylamine-PVA separating layer, 120–121
- Poly(vinylidene fluoride) (PVDF), 339
- substrate, 42–44
- Poly(vinyl pyrrolidone) (PVP), 184–185
- Polyvinyl sulfate membrane, 45–46
- Pore-flow mechanism, 90
- schematic diagram, 272, 272*f*
- Pore flow model, 3–4, 90, 90*f*, 359–361
- Porous and nonporous membranes, 106
- POSS. *See* Polyhedral oligomeric silsesquioxane (POSS)
- POSS-incorporated polymer systems, 206–207
- POSS – polymer nanocomposites, 208
- Predictive model, PV, 383–389
- chromatographic property, 384
 - contact angle, 384
 - interfacial thermodynamics, 384
 - polarity and solubility parameter, 383–384
- Pressure, pervaporation, 9
- Pressure swing reactive distillation (PSRD), 399
- Pristine graphene, 137. *See also* Graphene
- Protonated carboxyl acid groups, 47–48
- PSRD. *See* Pressure swing reactive distillation (PSRD)
- Pure liquid sorption, 369–373
- inverse gas chromatography method, 372–373
 - time-dependence of sorption, 370–371
 - time-lag experiment, 371

- PV. *See* Pervaporation
 PVA. *See* Poly(vinyl alcohol) (PVA)
 PVA-CS blended membranes, 42–44, 43*f*
 PV-assisted esterification reactions, 312
 PV-coupled fermentation process, 405
 PV-coupled laccase treatment, 405
 PV-esterification coupling process, 159
 PV membrane reactor (PVMR), 160
 PV separation index (PSI), 111
 Pyridine solution, 23–24, 24*f*
 Pyridinium, 83–84
 Pyromellitic dianhydride (PMDA), 180
- Q**
 Quantum confinement, 232
 Quantum dots, 231–232
 membranes, 147
 Quantum hall effect, graphene, 138–139
 Quaternary alkyl ammonium compounds, 83–84
 Quaternized chitosan and montmorillonite nanoclay (NaI-MMT), 91
- R**
 Raman spectrometry, 25
 RAST. *See* Real adsorbed solution theory (RAST)
 Real adsorbed solution theory (RAST), 268–269
 Reboiler heat transfer area, hybrid process parameter, 395
 Reduced graphene oxide (RGO) membrane, 61–62, 143–144
 Reverse microemulsion, 237–238
 Reverse osmosis, 175–176
 RF plasma synthesis technique, 253–254
- S**
 Scanning electron microscopy, 21
 Selectivity, intrinsic membrane properties, 5
 Selectivity rate, 309
 Self-assembled membranes, 190–192
 Self-assembly method, polymer nanocomposite pervaporation membranes, 178
 Separation efficiency, 143–144, 301–302
 Separation factor, 5, 110–111, 271, 357
 Silica, 7
 incorporated poly(vinyl alcohol) (PVA) membranes, 315–317
 membranes, 7, 58–59
 PAN/PEG membrane, 74–75
 polytetrafluoroethylene membrane, 72–73
 sol, 247–248
 Silicalite-1, aluminum-free zeolite, 266
 Silicalite-1/PDMS membrane, 290–291
 Silicate-1 hydrophobic zeolites, 7
 Silicone rubber blends, 17–18
 Silver nanoparticle-based polymer, 241
 Silver polymer-metal nanocomposites membranes, 248–249
 Silver salt of polyacrylate, 241–242
 Simulations, hybrid pervaporation process, 403–405
 Single-walled carbon nanotubes (SWCNTs), 113–114
 SiO₂-reinforced polyelectrolyte complexes (PECs) membranes, 7–8
 Si-O-Si stretching, 52–54
 S-O-C linkage, 42
- Sodium alginate, 6–8, 46–47
 chitosan/multiwall carbon nanotube membrane, 69–70
 membrane, 46–47
 Sodium carboxymethyl cellulose (NCCM), 144–145
 polyelectrolyte complex, 47–48
 Sodium 2-formyl benzene sulfonate polysiloxane (SBAPTES), 63–65
 Sol-gel synthesized membranes, 177, 192–195
 esterification and polycondensation reactions, 194–195
 heat-treated hybrid membrane, 194–195
 heat treatment, 194–195
 hybrid polymer inorganic membrane, 192–193
 operating conditions, 193–194
 TEOS, 192–193
 Sol-gel technique, 159, 236–237, 253–254
 Solubility, 367–368
 coefficient, 217, 271
 Solution-casting method, 188–189, 331–333
 Solution-diffusion mechanism, 89–90, 178
 schematic illustration, 212*f*
 Solution-diffusion model, 2–3, 89–90, 89*f*, 107–110, 110*f*, 361–363
 schematic diagram, 270, 271*f*
 water/alcohol mixture separation, 272
 Sorption, 110, 308, 361–362
 coefficient determination, 373–374, 374*t*
 equilibrium, 368
 selectivity, 2–3, 357
 Sp²-hybridized carbon atoms, 116
 Spinning technique, 278–279
 Spraying, 335
 Sputtering, 235

- Star-like polymer
nanocomposites, 208, 209*f*
- Sulfation of polyelectrolyte
membrane (S-PVS/CS),
45–46
- Sulfonated poly(styrene-
ethylene/ butylenes-styrene)
(S-SEBS) block copolymer
membrane, 183–184
- Sulfonation of polystyrene, 253
- Sulfonic acid functionalization,
63–65
- Sulfonized chitosan membrane,
63–65
- Sulfosuccinic acid (SSA)
membrane, 59–60
- Sulfuric acid, 55–58
hydrolysis, 19
strengthening, 55–56
- Superhydrophobic ZIF-7 pore
channels, 336–339
- Supported liquid membrane
(SLM), 160
- Surface diffusion, 360
- Surface hydrophilicity, 140–141
- Surface plasmon resonance
(SPR), 241–242
- Surfactant, 83–84, 235
- SWCNTs. *See* Single-walled
carbon nanotubes (SWCNTs)
- Swelling percentage degree, 112
- Synthesized sulfonated
polystyrene (SPS), 253
- Synthetic membranes, 313–314
- Synthetic polymers, 8–9
- T**
- TAC. *See* Total annual cost
(TAC)
- Temperature, pervaporation,
10–11, 358
- TEOS cross-linked chitosan
membrane coated on
polytetrafluoroethylene
substrate (TEOS/CH-PTFE),
72–73
- Tetrabutyltitanate (TBT), 253
- Tetraethoxysilane (TEOS), 177
- Tetrahydrofuran (THF), 42, 212,
214
- Thermal-sensitive compounds,
107
- Thermal stability, 59–60,
253–254
- Thermodynamics model,
364–365
- Thermodynamic vapor – liquid
equilibrium limitation, 109
- Thermoplastic block copolymer,
183
- THF. *See* Tetrahydrofuran (THF)
- 3-amino-
propyltriethoxysilane, 177
- Three-dimensional materials,
81–82
- Time-dependence of sorption,
370–371
- Time-lag experiments, 371, 372*f*
- Titania, 7
- Titanium dioxide (TiO₂)
membrane, 54–55, 253
- Titanium glycine-N,N-
dimethylphosphonate
(TGDMP), 253
- Titanium tetrachloride, 253
- Toluene-2,4-diisocyanate (TDI)
membrane, 60–61
- Toluene-n-heptane mixtures, 96
- Total annual cost (TAC),
394–395
- Total dissolved solids (TDS),
175–176
- Trade-off relationship, 17–18
- Transmission electron
microscopy (TEM), 24
- Transport mechanism,
polymer/clay
nanocomposites, 88
- Transport properties in
pervaporation (PV), 367–368
- Tray cost, hybrid process
parameter, 395
- 2,4,6-Triaminopyrimidine, 288*f*
- Trichloroacetic acid, 37
- Trifunctional organosilicon
monomers, 207–208
- Trimethyl silyl cellulose
(TMSC), 20–21
- Tri-n-octylamine (TOA), 160
- T-type zeolite, 265
- Tubular pervaporation
membrane, 183
- Tubular-type membrane,
278–279
- Two-dimensional (2D)
materials, 81–82
- U**
- Ultrafiltration, 106
- Ultrasonication, 277–278
- Ultrathin PVA membrane, 181
- Uncross-linked hybrid
membrane, 63–65
- Universal Testing Machine,
57–58
- Urea formaldehyde sulfuric acid
mixture (UFS), 42
- UV-vis absorption of PVA-AgNP,
242*f*
- V**
- Vacuum-driven membrane
process, 107
- Vacuum filtration method, GO
deposition, 190–191
- Vacuum pump, 108–109
- Vander Waals force, 82–83
- Vapor – liquid equilibrium
(VLE), 13
curve, 397
water/ acetic acid, 397, 398*f*
- Vapor-phase grown techniques,
153
- Vapor pressure difference,
108–109
- VBA. *See* Visual Basic for
Applications (VBA)
- Visual Basic for Applications
(VBA), 403–405
- W**
- Water/alcohol separation in
zeolite, mechanism,
266–275

- alcohol-selective zeolites, 264–266
- mixed matrix membranes and inorganic fillers, 270–275
- zeolite particles, 267–270
- Water-colloidal fullerenes, 164
- Water removal, 304–305
- Water-selective membranes, 109
- Water-soluble polymer, 235
- Water treatment
 - polyhedral oligomeric silsesquioxane-embedded polymeric systems, 220
- X**
- X-ray diffraction, 45
- X-ray photoelectron microscopy, 45–46
- X-ray photoelectron spectroscopy (XPS), 253
- Z**
- Zeolite, 7, 57–58
 - aspect ratio, 279–280
 - chabazite (CHA), 265
 - DDR, 265–266
 - Linde type A (LTA), 264–265
 - particles, separation
 - mechanism in, 267–270
 - and silica, 159
 - T-type, 265
 - type and characteristics, 266*t*
 - water and alcohol-selective, 264–266
 - ZSM-5, 266
- Zeolite 3A, 184–185
- Zeolite-based polymer nanocomposite membranes
 - compatibility, 279–287, 291
 - performances in pervaporation, 287–291, 289*t*
 - solution-diffusion mechanism, 264
 - water/alcohol separation in zeolite, mechanism, 266–275
 - mixed matrix membranes and inorganic fillers, 270–275
 - zeolite particles, 267–270
 - water and alcohol-selective zeolites, 264–266
 - zeolite-filled nanocomposite membranes, fabrication, 275–279
- Zeolite-filled polymeric membrane, 264, 275–279
- Zeolite – polymer MMMs, 281–282
- Zeolite/poly(vinyl) alcohol (PVA) membrane, 276
- Zeolitic imidazolate frameworks (ZIF-8) nanoparticle, 213–214
- Zero-dimensional (0D) nanomaterials, 81–82
- Zero field conductivity, graphene, 138–139
- Zero permeate pressure, 9
- ZIF-7/PTMPS MMM, 340
- ZIF-8/PTMPS MMM, 340
- Zinc oxide NPs, 237–238
- Zirconia, 7
- Zn(BDC)(TED)_{0.5}, 339–340
- ZSM-5, 266
- Zwitter-ionic polymers, 146

POLYMER NANOCOMPOSITE MEMBRANES FOR PERVAPORATION

Sabu Thomas, Soney C. George and Thomasukutty Jose

Polymer Nanocomposite Membranes for Pervaporation assesses the recent applications in pervaporation performance of polymer nanocomposites of different length scales. Polymer nanocomposite membranes are suitable for use in pervaporation separation, because of their stability and chemical resistivity due to their nanoparticle reinforcement. Pervaporation is one of the best techniques to separate azeotropic mixtures, close-boiling liquid mixtures, and for the desalination process.

The book discusses the effects of nanofillers and their dispersion, different types of polymers, and nature of nanofillers in the pervaporation process. The book explores how the different properties of varieties of nanocomposite materials make them better for use in different types of liquid mixture separations, and also discusses the challenges of using different nanocomposites for this purpose effectively and safely. In particular, polymer nanocomposite membranes for different pervaporation applications and their correlation with nanoscale dispersion, filler–polymer interactions, and morphology are addressed.

This is an important reference source for materials scientists, chemical engineers, and environmental engineers who want to learn more about how polymer nanocomposites are being used to make the pervaporation separation process more effective.

Key Features

- Explores the progress that has been made in recent years in using polymer nanocomposites to enhance the pervaporation separation process;
- Discusses the different properties of a variety of nanocomposites, in assessing the situations, in which they should best be used;
- Outlines the major challenges to using polymer nanocomposites in the pervaporation separation process safely and effectively;
- Insights into the theoretical modeling of the pervaporation membranes.

Prof. Sabu Thomas is currently Vice Chancellor of Mahatma Gandhi University and Professor of Polymer Engineering and Nanotechnology, Kerala, India.

Dr. Soney C. George, Dean Research and Director Centre for Nanoscience and Technology, Amal Jyothi College of Engineering, Kanjirappally, Kerala, India.

Dr. Thomasukutty Jose is the Assistant Professor of Chemistry at Amal Jyothi College of Engineering, Kanjirappally, India.



ELSEVIER

elsevier.com/books-and-journals

Technology and Engineering/
Material Science

ISBN 978-0-12-816785-4



9 780128 167854